Journal Pre-proof

Volcanic glass leaching and the groundwater geochemistry on the semi-arid Atlantic island of Porto Santo

Maria Teresa Condesso de Melo, Raghwendra Narayan Shandilya, João Baptista Pereira Silva, Dieke Postma

PII: S0883-2927(19)30277-X

DOI: https://doi.org/10.1016/j.apgeochem.2019.104470

Reference: AG 104470

To appear in: *Applied Geochemistry*

Received Date: 16 May 2019

Revised Date: 13 November 2019

Accepted Date: 13 November 2019

Please cite this article as: Condesso de Melo, M.T., Shandilya, R.N., Silva, Joã.Baptista.Pereira., Postma, D., Volcanic glass leaching and the groundwater geochemistry on the semi-arid Atlantic island of Porto Santo, *Applied Geochemistry* (2019), doi: https://doi.org/10.1016/j.apgeochem.2019.104470.

second revision submitted to Applied Geochemistry

Volcanic glass leaching and the groundwater geochemistry on the semi-arid Atlantic island of Porto Santo.

Maria Teresa Condesso de Melo[1], Raghwendra Narayan Shandilya[1,4], João Baptista Pereira Silva[2,3], Dieke Postma[4*]

[1]CERIS, Instituto Superior Técnico, Universidade de Lisboa, Av. Rovisco Pais, 1049-001 Lisboa, Portugal

[2]Madeira Rochas, Avenida Arriga 75, Conjunto Monumental do Infante, Apartamento 506, 9000 - 060 Funchal, Madeira, Portugal

[3]GEOBIOTEC, Geosciences Department, University of Aveiro, Campus de Santiago, 3810-193 Aveiro, Portugal.

[4]present address: KIST School, Korea University of Science and Technology (UST), Seoul, South Korea

[5]Dept. of Geochemistry, GEUS, Øster Voldgade 10, DK1350 Copenhagen, Denmark

[*]Corresponding author: diekepostma@gmail.com

Declarations of interest: none

Abstract

The groundwater chemistry of the semi-arid volcanic island of Porto Santo, part of the Madeira archipelago, Atlantic Ocean, was investigated. Generally, the groundwater was brackish, containing 2-10 mol % seawater. Groundwater with up to 20 mM alkalinity and a Na enrichment of up to 30 mM, as compared to the Na concentration predicted by the seawater Na/Cl ratio, was found in the main aquifer. Also notable are the high concentrations of F (up to 0.3 mM), B (up to 0.55 mM), As (up to 0.35 µM), all in excess of WHO recommendations, as well as up to 6 µM V. Geochemical modeling, using the PHREEQC code, was used to explore different scenarios that could explain the genesis of the observed bulk groundwater chemistry. First, a model for aquifer freshening with the displacement of resident seawater from the aquifer by infiltrating freshwater, was tested. This scenario leads to the development of $NaHCO_3$ waters as observed in many coastal aquifers. However, the measured alkalinity concentration in the groundwater was far higher than the concentration predicted by the freshening model. In addition, the behavior of modelled pH and P_{CO2} were at variance with their distributions in the field data. The second model explored the possible effect of volcanic glass leaching on the groundwater chemistry. Using insight derived from studies of volcanic glass surface alteration as well as experimental work on water-volcanic glass interactions, a geochemical model was developed in which the exchange of H^+ for Na^+ on the volcanic glass surface is the main mechanism but the exchange of other cations on the volcanic glass surface is also included. The uptake of H^+ by the glass surface causes the dissociation of carbonic acid, generating bicarbonate. This model is consistent with the local geology and the field data. It requires, however, volcanic glass leaching to occur in the unsaturated zone where there is an unlimited supply of CO_2. The exchange reaction of H^+ for Na^+ is confined to the surface layer of volcanic glass as otherwise the process becomes limited by slow solid state diffusion of H^+ into the glass and Na^+ out of the glass. Therefore, volcanic ash deposits, with their high volcanic glass

surface areas and matrix flow, are the aquifers where this type of high $NaHCO_3$ waters can be expected, rather than in basalts, which predominantly feature fracture flow. The trace components F, B, As and V are believed to originate from hyaloclastites, consisting of predominantly (90%) of trachy-rhyolite volcanic glass. Although stratigraphically older than the main calcarenite aquifer, topographically they are often located at higher altitudes, above the phreatic level and located along the main recharge flow path. In addition, the semi-arid climate conditions provide a long groundwater residence time for the reactions as well as limited aquifer flushing.

1. Introduction

The islands of Macaronesia in the Atlantic Ocean, the Canaries, Cape Verde, Azores and the Madeira archipelago, are predominantly volcanic in origin (Burke and Wilson, 1972; Ferreira et al. 1988; Holik et al., 1991; Carracedo, 1999; Geldmacher et al., 2001, 2006; Patriat and Labails, 2006). However, their groundwater resources and the groundwater chemistry varies greatly depending on factors like climate, geology and relief. It ranges from islands with abundant precipitation such as the Azores (Cruz et al., 2014) over the semi-arid Canaries (Herrera and Custodio, 2014; Custodio et al., 2016) and the desert-like conditions on the Cabo Verde islands (Heilweil et al., 2006, 2009, 2012; Condesso de Melo et al., 2008; Carreira et al., 2010). The Madeira archipelago is an intermediate case. The main island Madeira rises to an altitude of 1861 m and gets abundant precipitation (Prada et al., 2005). However, Porto Santo island, located 45 km further northeast, only rises 517 m above sea level, gets therefore less precipitation and is semi-arid. As a result, the groundwaters of Madeira island are dilute with short residence times of water in the aquifer (Prada et al., 2005), while Porto Santo has groundwater with a much higher solute content (Condesso de Melo et al., 2008). There is a considerable concern of how climate change will influence the water resource in Macaronesia. Current model predictions indicate that for Madeira and the Canaries the predominant winter precipitation will decrease by respectively up to 22 % and 37% before the year 2100 (Cropper, 2013; Cropper and Hanna, 2014). In order to assess how these changes may affect the chemical composition of the groundwater, a proper understanding of the controlling geochemical processes is required.

Weathering of volcanic glass is a process of particular importance during the early stages of basalt weathering, both due to faster dissolution rates of glass as compared to minerals but also due to the relatively high exposed surfaces areas of the glass (Gislason and Oelkers 2003). Volcanic glass weathering has been studied in relation to soil development with bulk transformation into minerals like halloysite and smectites (Dubroeucq et al., 1998; Mirabella et al., 2005). Volcanic

glass weathering has also been studied as a natural analogue to evaluate the resistance of artificial radioactive waste glasses against corrosion (Lutze et al., 1985; Crovisier et al., 1992; Magonthier et al., 1992; Vernaz and Dussossoy, 1992). In recent years the potential storage of CO_2 in basaltic rocks on Iceland has been investigated and here it was found that the interaction between the injected CO_2 and the basalt results in the extensive precipitation of carbonate minerals (Matter et al., 2016; Snæbjörnsdóttir, et al., 2017, 2018)

The initial stage of low temperature volcanic glass alteration consists of leaching of the glass surface and has been studied using analysis of volcanic glass surfaces from Iceland (Magonthier et al., 1992), the Azores (Mungall and Martin, 1994) and Gran Canaria (Cousens et al., 1993). During the meteoric exposure of the volcanic glass surface, water diffuses into the glass surface and creates a reaction zone enabling H_3O^+ to enter and exchange Na^+ for H^+. The H^+ ion interdiffuses with particularly Na^+, without devitrification (White, 1983; Magonthier et al., 1992; Vernaz and Dussossoy, 1992; Mungall and Martin, 1994; Fiore et al,, 1999). Magonthier et al., 1992 showed that upper Pleistocene obsidian from Iceland had the upper 100 nm of the surface layer depleted in Na and enriched in H. With increasing depth below the glass surface, the concentration of H^+ rapidly decreased as it is controlled by solid state diffusion of H_3O^+ into the glass. In good accordance, Mungall and Martin (1994) did calculate a diffusion coefficient for Na^+ out of the trachyte glass of 1.8-6.1 x 10^{-19} cm^2/s, and White (1983) 6.1 x 10^{-19} cm^2/s for obsidian, both in the range expected for solid state diffusion. The result of this diffusion controlled Na^+ / H^+ exchange process is that it initially is fast but will come to almost a standstill as it moves away from the glass surface. The initial stage of volcanic glass leaching with Na^+/H^+ exchange is fast enough to significantly influence the water chemistry (Truesdell, 1966; White, 1983) and may result in high $NaHCO_3$ groundwater (Truesdell, 1966; White, 1979; White et al., 1980). Here, we try to combine the insights obtained from solid phase chemistry and experimental evidence on water-volcanic glass

112 interactions into a quantitative geochemical model to interpret how volcanic glass H^+/Na^+ surface
113 exchange could have resulted in high $NaHCO_3$ groundwater on the semi-arid island Porto Santo.

114

115 **2. Geological and Hydrogeological setting**

116 Porto Santo is a volcanic island, part of the Madeira archipelago that is located in the Atlantic
117 Ocean, west of southern Europe and northern Africa. It is a small island (42.2 km^2) extending
118 between 32° 59' and 33° 07' N and 16° 16' and 16° 24' W. The island is quite a flat and
119 characterized by two distinct regions; the rugged northeast part with some of the highest peaks, up
120 to 517 m high, and the southwest consisting of a low lying coastal plain with a nine-kilometer-long
121 white sand beach. The island has a semi-arid climate and soils for agriculture are sandy and poor in
122 nutrients. Freshwater resources very scarce and the island relies mostly on groundwater for
123 irrigation and on seawater desalination for public water supply.

124

125 *2.1 Geology*

126 The volcanic activity under the island of Porto Santo was initiated on the sea bottom at 3000 m
127 depth over a hot spot (Mata et al., 1998). The oldest volcanic activity is dated 16 mill years B.P. and
128 the latest volcanic activity took place 10 mill years ago (Ferreira et al., 1988; Ferreira and Neiva,
129 1996). The geological formations of Porto Santo are divided into two main rock types (Fig. 1):
130 extrusive igneous rocks, mainly basalts, directly linked to the volcanic origin of the island itself;
131 and sedimentary rocks, that cover about one third of the island and include fossiliferous limestone
132 breccias, sandy limestones and marls, carbonate eolianites, sand dunes, limestone crusts and
133 alluvium, slope and beach deposits (Ferreira and Neiva, 1996). The volcanic rocks include a
134 submarine sequence with the oldest rocks (basaltic and trachybasaltic flows interlayered with

pyroclastites and hyaloclastites, and other volcaniclastic deposits); and a subaerial sequence composed with mainly basaltic clastolavas (trachytic rocks, in the form of domes and lava flows, mugearites and hawaiites) that overly subaerial basalts (Ribeiro & Ramalho, 2010). The carbonate sediments show frequent paleosol features such as caliche reflecting arid conditions, as does the occurrence of montmorillonite as a weathering product of the volcanic rocks.

2.2 Hydrogeology

The low permeability volcanic rocks dominate Porto Santo in the north and south-western parts (Fig. 1) and give rise to steep slopes that promote surface runoff and limits groundwater recharge and availability. Carbonate eolianite deposits and coastal sands are present in the western and central part of the island and have good aquifer properties but limited rainfall and high evapotranspiration rates constrain the recharge processes.

The average annual rainfall is less than 500 mm (IPMA, 2017), occurring often as short heavy events during winter that may produce flash floods and strong landscape erosion (locally called ‘badlands’). Direct evaporation from open pan yielded average of 1471 mm per annum. Indirect estimates using the Penman (1948) and Thornthwaite (1948) equations gave respectively 1887 and 889 mm per annum. The average monthly evaporation values for all measured months, and all methods, are higher than the average monthly precipitation. Thus, all three evapotranspiration values conclude to a water deficit on the island. The groundwater recharge calculated using the chloride mass balance approach yields 11.4 mm per annum (Shandilya, 2017). The regional management plan of hydrographic network in archipelago of Madeira (APA, 2016) reports an average annual recharge volume of 20.4 mm.

Four major hydrogeological units have been defined in the island (Ferreira & Neiva, 1996): (1) carbonate eolianites; (2) beach sands; (3) eruptive volcanic rocks; and, (4) weathered volcanic rocks with clay (Fig. 1). The carbonate eolinites and the beach sands form the most permeable and productive aquifer units of about 30 to 50 m deep; while the volcanic formations in the form of basalts, rhyolite and trachyte are fractured and weathered at places but infiltration and transmissivity is very limited. The geological contacts between sedimentary and volcanic formations provide preferential pathways for a number of springs, which are mainly used for crop irrigation. In terms of conceptualization of groundwater flow circulation, it can be said that rainwater is the main source of groundwater recharge but effective recharge is <5% of the total annual rainfall due to evapotranspiration. The groundwater circulates following the topographic gradients to the central part of the island and to the coast. In the volcanic rocks, water infiltrates and circulates through fractures and dykes discharging to main low laying aquifer units (carbonate eolianites and beach sands) and through springs.

The submarine volcanic formations that cooled very fast when extruded on the sea floor contain connate seawater and this may justify the high groundwater salinities observed in some volcanic formations located far away from the coast (Supplementary Materials Fig. A1.1). In the case of the hyaloclastite formation, the fast cooling processes caused them to consist of about 90% trachy-rhyolite volcanic glass. Hyaloclastites are very abundant on the island and have a great importance for the enrichment of some elements in groundwater (As, F, Ni). Although stratigraphically older than the calcarenite eolianite formation (main aquifer), topographically they are often located at higher altitudes above the phreatic level and are along recharge flow path reacting with infiltrating water. This means that water circulates through the hyaloclastites through fractures and along dykes (trachyte and basalt) and discharges into the calcarenite eolianite formation.

3. Data Collection and Analysis

Groundwater samples were collected from all major geological formations during various field campaigns (Fig. 1). Twenty samples were taken from calcarenite aquifers, 15 samples are from hyaloclastite deposits, 8 samples are from submarine basalt deposits, 3 from weathered pyroclasts deposits, and there is one sample in each of the following, tuff, pillow lava, trachyte. The total dataset comprises 52 samples of which 36 were collected and analyzed during previous campaigns which are reported in Condesso de Melo et al., (2008) and Silva et al., (2008). The remaining samples were collected during the spring of 2017 (Shandilya, 2017). Because of the low infiltration rate and therefore the long groundwater residence time, the results of the different sampling campaigns are considered comparable. The sampling sites include springs, shallow aquifer wells and boreholes, some with a large diameter, spatially distributing over the whole island. A multiport flow-through cell connected in-line to the sampling points was used to measure pH, temperature (T), specific electrical conductance (SEC) and dissolved oxygen (DO). Water samples were taken from the discharge point during pumping, once stabilization of the principal field parameters: pH, temperature (T), specific electrical conductance (SEC) and dissolved oxygen (DO) was observed. Water samples were on-site filtrated through 0.45 µm membrane filters using a syringe. On-site measurements also included the determination of alkalinity (quoted as HCO_3^-) by acid titration using standard colorimetric titration HACH® kit method. The method involved titrating 100 mL of the sample with sulphuric acid 1.6 N to pH~4.5 using a bromocresol green indicator. The analysis of major, minor and trace elements of the samples for all field campaigns was performed by ICP/MS at the Activation laboratories in Ontario (Canada). Electroneutrality was used as a quality control for major components, and ionic mass balances with errors between –10% and +10% were considered to be acceptable, and 57% of the analyses were within ± 5%. Speciation calculations and

geochemical modeling were carried out using PHREEQC-3 (Parkhurst and Appelo, 2013) and the database PHREEQC.DAT.

4. Results

4.1. Major groundwater components

The groundwater on the island of Porto Santo is oxic with an O_2 concentration in the range 0.06 to 0.27 mM (1.86-8.7 mg/L) and has a temperature in the range 17-22 ^{o}C. The pH of the groundwater spans from 6.6 to 9.2 with the large majority of the samples in the range 7.5-8.5. Figure 2 displays the major ion water chemistry, while indicating the sampled aquifer type (Fig. 2c) as well as the seawater ion/Cl molar ratios, using the seawater composition of Turekian (1968). The majority of the samples contains between 2 and 10 mol % of 35 ‰ seawater, as judged from their chloride content (Fig. 2). The distribution of the Cl concentration over the island (Supplementary Material Figure A1.1) is more or less random with some of the highest values in the centre of the island. The Br/Cl molar ratio (Supplementary Material Figure A1.2) is very close to that of seawater. Almost all waters (Fig. 2a) exceed the WHO guidelines for Cl (250 mg/L ≈ 7 mM) as well as for Na (200 mg/L ≈ 8.7 mM). The Na concentration is up to 30 mM higher than predicted from the seawater Na/Cl ratio. Also notable is the strong enrichment, of up to 20 mM, in alkalinity as compared to seawater (Fig. 2b). There is no major difference in Na or alkalinity concentration between carbonate and volcanic aquifers even though the highest contents were measured in volcanic aquifers. Neither is there a significant difference in concentration between the various volcanic rock types. For Ca, the groundwater in carbonate aquifers is with few exceptions conform the Ca/Cl ratio in seawater (Fig. 2c). In volcanic aquifers the Ca content is, at lower Cl concentrations, well below the Ca/Cl seawater ratio while for higher Cl concentrations the Ca/Cl ratio is much higher. Again these

differences are not related to the type of volcanic aquifer rock. Finally for Mg (Fig. 2d), almost all samples, except for those with the highest Cl, are depleted with Mg as compared to the Mg/Cl seawater ratio. The WHO guideline for Mg of 50 mg/L (≈ 2.1 mM) is exceeded in several samples, which also have a high Cl concentration.

Both for Sr (Fig. 3a) and K (Fig.3b) the groundwater from carbonate aquifers tends to be enriched as compared to the ion/seawater ratio while the reverse is the case for the volcanic aquifers. However, at a high Cl concentration, where also high Ca was found (Fig. 2c), several samples show a very high Sr concentration (Fig. 3a). The sulfate concentration (Fig. 3c) is generally higher than the seawater line with nearly half of the samples exceeding the WHO guideline of 250 mg/L (≈ 2.6 mM) while there is no significant difference between carbonate and volcanic aquifers. Finally, nitrate (Fig. 3d) is generally below the WHO guideline of 50 mg/L (≈ 0.8 mM) but in a few cases more than 1 mM NO_3 is found reflecting the sparse agricultural activity.

4.2. Contaminant trace components F, B, As and V

Most of the groundwater contains a fluoride in excess of the WHO limit of 1.5 mg/L (≈ 0.08 mM) with the concentration becoming as high as 0.3 mM (Fig. 4a) and fluorosis (dental mottling) is commonly found on the island (Mendes, 2006). No significant difference is found between the fluoride concentration in carbonate or volcanic aquifers. Boron is the only substance discussed here where the European Community (1998) guideline (1 mg/L ≈ 0.1 mM) deviates from the WHO guideline (0.5 mg/L ≈ 0.05 mM) guideline. The groundwater reaches a boron concentration of up to 0.55 mM (Fig. 4b) exceeding both guidelines in nearly all samples. In addition, the boron concentrations are much higher than predicted by the seawater B/Cl ratio and generally B tends to be higher in carbonate aquifers than in volcanic aquifers although there is an overlap. Finally, there

are a number of occurrences where the WHO guideline for arsenic (10 µg/L ≈ 0.13 µM) is exceeded (Fig. 4c). The vanadium concentration (Fig.4d) is in most cases < 1 µM but in several volcanic aquifers values of up to 6 µM are found. There is no WHO, nor EU, guideline for vanadium in drinking water but in Italy the Superior Council of Health (SCH, 2001) has given a guideline value for vanadium in drinking water of 50 µg/L ≈ 1 µM. As displayed in Fig. 4d, this guideline is exceeded in a number of wells. The complete dataset of chemical groundwater analyses has been appended as the file: Porto Santo_groundwater chemistry.xlsx

4.3. Mineral equilibria

Figure 5a shows the calculated activities of Ca^{2+} and CO_3^{2-} in the groundwater and the solubility lines for the two $CaCO_3$ minerals, calcite and aragonite. As shown in Fig. 5a, aragonite has a higher solubility than calcite. The groundwater data plots around the solubility lines for the two minerals, suggesting overall an equilibrium control of dissolved carbonate and Ca by $CaCO_3$ equilibria. There is a weak tendency of carbonate aquifers being more supersaturated than the volcanic aquifers. Part of the observed supersaturation can be an artefact from sampling large diameter wells, tunnels and galleries, where CO_2 degassing and mixing can occur, causing the pH to increase and as a result the water may become more supersaturated with respect to $CaCO_3$ than it was in situ in the aquifer. Aragonite is particularly abundant in recent carbonate sediment and can contain much more Sr than calcite (Appelo and Postma, 2005). The high groundwater Sr concentration (Fig. 3a) may therefore indicate recrystallization of aragonite into the more stable calcite.

Figure 5b shows the saturation state of the groundwater with respect to fluorite (CaF_2). All groundwater samples are subsaturated towards fluorite and there is no significant difference between carbonate and volcanic aquifers. There is, however, an overall tendency that waters high in

F^-, are low in Ca^{2+} and vice versa. Again, one should bear in mind that sampling from large diameter wells and galleries may cause mixing of waters with a different composition which will influence the saturation state. For silica (Fig. 6), the concentration reaches 1.5 mM with the highest values found in the volcanic aquifers which indicates that weathering of volcanic glass plays a role. All groundwaters are supersaturated with respect to quartz (Fig. 6) and all volcanic aquifer samples are supersaturated with respect to chalcedony but subsaturated with respect to amorphous silica. Similar Si concentrations were found by Gislason and Eugster (1987) in basalts on Iceland. Finally for gypsum (not shown), the groundwater is always subsaturated by more than an order of magnitude.

5. Discussion

The groundwater chemistry of the island Porto Santo displays a number of different influences. First off all there is a distinct seawater component which may originate either from seawater captured in the rocks when submerged under sea-level, or present day seawater input as sea-spray and aerosols. The distribution of Cl over the island (Supplementary Material Figure A1.1) shows no clear pattern and has some of the highest values in the centre of the island where it probably is released from connate water in hyaloclastites. However, the seawater component does never exceeds 10 %. Secondly, there is not a big difference in the water chemistry of carbonate and volcanic aquifers and neither are there major differences between the different volcanic aquifer types. This is due to the complex hydrogeology with groundwater flowing from the topographic higher volcanic areas in the NE and SW of the island (Fig. 1) into the lower carbonate basin located in the centre (Shandilya, 2017). In addition, the carbonate sediments contain up to 10 % grains of volcanic origin (Silva, 2002). Particularly the higher Si concentration in volcanic rock aquifers

297 indicates that weathering of volcanic rocks is also important. Key features to be explained are the
298 very high alkalinity and Na^+ concentrations which are in large excess of the seawater Na/Cl ratio,
299 and the presence of a suite of trace contaminants like F, As, B, V. In the following, we will first
300 discuss the overall processes on the major component water chemistry and thereafter try to place the
301 occurrence of the contaminants into the picture.

302

303 *5.1. Aquifer Freshening*

304 The occurrence of $NaHCO_3$ groundwater is often attributed to freshening conditions in aquifers
305 (Stuyfzand, 1993; Walraevens and Cardenal, 1994; Appelo, 1994; Condesso de Melo, 2002; Appelo
306 and Postma, 2005; Postma et al. 2009). Here we explore if aquifer freshening could be a possible
307 explanation for the occurrence of $NaHCO_3$ groundwater on Porto Santo.

308 In the classical aquifer freshening scenario, the resident seawater in the aquifer is
309 displaced by incoming freshwater. In contact with seawater, the sediment exchanger will be rich in
310 adsorbed Na^+, while the incoming freshwater normally is dominated by Ca^{2+} and HCO_3^-, due to
311 equilibrium with $CaCO_3$. The Ca^{2+} in the incoming solution will exchange with adsorbed Na^+,
312 causing the Ca^{2+} concentration to decrease:

313 $$½Ca^{2+} + Na\text{-}X \rightarrow ½Ca\text{-}X_2 + Na^+ \quad (1)$$

314 The decrease in the Ca^{2+} concentration will cause sedimentary $CaCO_3$ to dissolve:

315 $$CaCO_3 + H_2CO_3 \rightarrow Ca^{2+} + 2HCO_3^- \quad (2)$$

316 Which will initiate further displacement of Na-X by Ca^{2+}. The result of the two coupled reactions
317 will be water enriched in both Na^+ and HCO_3^-. In the case of Porto Santo a freshening scenario
318 could be envisioned with the island originally submerged below sealevel, while upon emergence

above sealevel, freshwater infiltration slowly displacing the seawater from the aquifer. Since Porto Santo groundwaters presently only contains up to 10 mol % seawater, it would in this scenario represent the distal part of the freshening front. As shown in Fig. 2, both Na^+ and HCO_3^- concentrations are strongly elevated as compared to the seawater Na/Cl and HCO_3/Cl ratios and therefore at least qualitatively consistent with a freshening scenario.

To explore the freshening scenario more quantitatively we have build a PHREEQC model. In short, the model consist of a sediment column filled with seawater equilibrated with aragonite and a cation sediment exchanger. Through this column freshwater is transported, consisting of water equilibrated with aragonite at a $P_{CO2} = 10^{-2}$ which is close to that of the groundwater samples. The PHREEQC input file and the full results are given in Supplementary Materials A3. During the model run, Na^+ is displaced from the exchanger by Ca^{2+} and alkalinity increases due to carbonate dissolution causing the Na/Cl and Alk/Cl ratios to increase. These increases, as predicted by the PHREEQC model can be compared with the groundwater observations (Fig. 7). The comparison shows that the measured groundwater Na/Cl and HCO_3/Cl ratios are much higher than what is predicted by the PHREEQC freshening model and any attempt to diminish the disagreement by adjusting model parameters within reasonable limits did fail. Also the pH and P_{CO2} predicted by the model are at variance with groundwater observations since the PHREEQC model (Fig. 7) predicts increasing pH and decreasing P_{CO2} towards low Cl concentration, which is not seen in the groundwater data. The inevitable conclusion is therefore that aquifer freshening is not a satisfactorily quantitative explanation for the Porto Santo groundwater chemistry.

5.2. Volcanic glass alteration

342 Leaching of the volcanic glass surface with exchange of H^+ for Na^+ has been suggested as a
343 mechanism leading to the development of sodium bicarbonate rich groundwater (Truesdell, 1966;
344 White, 1979; White et al., 1980), and here we examine this process as a possible cause for the
345 observed enrichment of the Porto Santo groundwater by Na^+ and HCO_3^-. An alternative explanation
346 could be the bulk weathering of volcanic glass and basalt with incongruent dissolution of the parent
347 rock and the precipitation of secondary phases like smectites, zeolites and carbonates. The
348 precipitation of secondary phases like smectites, zeolites or carbonates may preferentially remove
349 bivalent ions like Ca and Mg as compared to Na (White et al, 1980; Crovisier et al., 1992; Flaathen
350 et al., 2009). In the compilation of volcanic glass compositions of Wolf-Boenish et al. (2004) the
351 molar Ca/Na ratio ranges from 0.3 to 9.6 with more than 2/3 of the samples having a Ca/Na > 1. For
352 Mg the data of Wolf-Boenish et al. (2004) shows a molar Mg/Na ratio between ranges from 0.01
353 and 6.3 with more than 2/3 of the samples having a Mg/Na > 0.7. For comparison, Flaathen et al.
354 (2009) reported spring water in basalts on Iceland with molar ratios for Ca/Na of 1-2 and Mg/Na
355 0.1-0.5 as the result of weathering. The Porto Santo groundwater, however, features up to 20 mM
356 Na, but almost no Ca in excess of the seawater contribution, except for a few samples, and in most
357 samples there is a deficit in Mg as compared to the seawater contribution (Fig. 2d). Therefore, if
358 this water predominantly were the result of incongruent bulk dissolution of volcanic glass, then it
359 would require an extremely more effective selective removal of Ca and Mg than observed by
360 Flaathen et al. (2009). Our preferred interpretation is consequently that the high Na^+ and HCO_3^-
361 concentrations primarily are the result of H^+ /Na^+ surface exchange on the volcanic glass surface as
362 explained in more detail below and which is supported by surface analysis of volcanic glass
363 occurring in the field (Magonthier et al., 1992; Mungall and Martin, 1994).

364 There is experimental evidence for a fast exchange reaction between solutes and the
365 glass surface that may influence the water chemistry. Truesdell (1966) constructed electrodes from

366 a number of natural and synthetic grounded glasses and used these to determine the ion exchange
367 properties of the glasses. The results revealed major variations between the different glasses but all
368 obeyed the following selectivity sequence $2H^+ > 2K^+ > 2Na^+ > Ca^{2+} \geq Mg^{2+}$. White 1983 showed
369 experimentally that depletion of surface Na^+ from volcanic glass and Na^+ release to the aqueous
370 solution occurs in a matter of hours. The surface reaction as it affects the water chemistry may be
371 written as:

372 $$Na\text{-}X + H^+ \rightarrow H\text{-}X + Na^+ \quad (3)$$

373 Combining this reaction with the dissolution of CO_2 and the dissociation of carbonic acid results in:

374 $$Na\text{-}X + CO_2 + H_2O \rightarrow H\text{-}X + Na^+ + HCO_3^- \quad (4)$$

375 Accordingly, this reaction scheme results in the formation of $NaHCO_3$ water. A consequence of this
376 reaction scheme is that the exchange process needs to take place in the presence of continuous CO_2
377 replenishment, like in the soil or in the unsaturated zone with respiration or organic matter
378 degradation. If there is no CO_2 replenishment then reaction (3) will increase the pH, decreasing the
379 H^+ concentration, and therefore the reaction will stop.

380 We have investigated surface exchange on volcanic glass as a possible explanation for
381 the composition of Porto Santo groundwater by modelling the ion exchange reaction between a
382 volcanic glass exchanger, initially filled with Na^+, in contact with dilute seawater. The Na-X
383 exchanger is equilibrated with water containing different amounts of sea-salt at a constant P_{CO2} of
384 $10^{-2.25}$, corresponding to the median P_{CO2} of the groundwater (Fig. 8). The PHREEQC input file is
385 listed in Supplementary Materials A4. We here use the notation as given in the PHREEQC database
386 where ion exchange reactions are described as half reactions with a strength relative to Na^+ (Appelo
387 and Postma, 2005):

388 $$Na^+ + X^- \leftrightarrow Na\text{-}X \quad \text{with } \log K_{Na\text{-}X} = [Na\text{-}X]/[Na^+][X^-] = 0 \quad (5)$$

389 is defined as the reference and

390 $H^+ + X^- \leftrightarrow H\text{-}X$ with $\log K_{H\text{-}X} = [H\text{-}X]/[H^+][X^-]$ (6)

391 as the competing reaction.

392 The procedure is to fit the model to the field data for primarily the groundwater Na^+ concentration
393 and the alkalinity by adjusting the association constant $K_{H\text{-}X}$. The P_{CO2} is kept at a constant value of
394 $10^{-2.25}$ in correspondence with the field data (Fig. 8). However, this procedure also needs a value for
395 the total number of exchange sites, X^-, on the glass surface. The number of exchange sites is not
396 well defined and the choice of value will affect the $K_{H\text{-}X}$ needed to model the field data as well as
397 the amount of surface Na-X sites that is being replaced by mainly H-X. We have modelled the data
398 for three feasible values for the X^- surface concentration, 1 mol/L, 0.1 mol/L and 0.05 mol/L
399 expressed relative to contacting groundwater. For comparison a montmorrilonite with 1000 meq/kg
400 (Appelo and Postma, 2005) recalculates to 6.3 mol/L contacting porewater using a porosity of 0.3
401 and bulk density of 1.86 g/cm^3. Likewise, a kaolinite of 30 meq/kg corresponds to 0.2 mol/L
402 contacting groundwater.

403 Figure 8 shows the field data together with the model fits while Table 1 presents the
404 fitted association constants. The field data can be modelled equally well for all three surface site
405 concentrations (Fig. 8) using the different constants listed in Table 1. The model both can explain
406 the very high measured Na and alkalinity concentrations and is also consistent with the measured
407 pH. The release of Na^+ from volcanic glass and the associated build-up of alkalinity is in the model
408 controlled by the displacement of Na-X by mainly H-X. The main differences between model and
409 field data are caused by samples that deviate in P_{CO2} from the value used in the model. Thus, a
410 number of samples at low Cl concentration have a particularly high P_{CO2} causing the pH and
411 alkalinity to become lower.

412 For a high exchange site concentration only a small fraction of the surface Na-X needs
413 to be replaced to produce the aqueous Na^+ and alkalinity concentration, while for a lower exchange
414 site concentration a greater fraction of Na-X must be replaced to obtain the same Na^+ and alkalinity
415 concentration. Therefore, the K_{H-X} is larger for a low concentration of X^- than for a higher X^-. In all
416 cases the H-X association constant is very high which is required in order to displace Na-X on the
417 surface because the H^+ concentration always is very low as compared to the Na^+ concentration. To
418 assess what a reasonable exchange site concentration could be, the amount of Na-X displaced from
419 the glass surface as calculated by the model (Table 1), can be compared with field measurements.
420 Magonthier et al. (1992) showed that upper Pleistocene obsidian from Iceland had about half of the
421 surface sites of Na^+ replaced by H^+. Mungall and Martin (1994) showed that altered pumice from
422 the Azores had lost 33-43 % of its Na. If these surface concentrations also apply to Porto Santo,
423 then they indicate that the surface exchange site concentration of Porto Santo volcanic glass is near
424 the low end and the log K_{H-X} near the high end of the range given in Table 1.

425 The surface sites also function as an ion exchanger taking up ions from the solution as
426 demonstrated by Truesdell (1966). Seawater is high in Mg^{2+} and the depletion of the groundwater as
427 compared to the seawater Mg/Cl ratio suggests the uptake of Mg by the glass surface from seawater
428 as given by the reaction:

429 $$Mg^{+2} + 2X^- \leftrightarrow Mg\text{-}X_2 \quad \text{with} \quad K_{MgX2} = [Mg\text{-}X_2]/[Mg^{2+}][X^-]^2 \qquad (7)$$

430 While on a exchanger like clay mineral, multivalent ions are always much stronger adsorbed than
431 monovalent ions (Appelo and Postma , 2005), this is not the case for the volcanic glass surface
432 where divalent ions actually are adsorbed more slightly (Truesdell, 1966). To fit our field data (Fig.
433 8) we therefore have to lower the association constant for $Mg\text{-}X_2$ (Table 1) by several orders of
434 magnitude as compared to standard values for clay (Appelo and Postma, 2005). In addition, we

435 have included Ca^{2+} in the exchange model and following Truesdell (1966) we have included $Ca\text{-}X_2$
436 in the model using the same log K value as for MgX_2 (Table 1).

437 $$Ca^{+2} + 2X^{-} \leftrightarrow Ca\text{-}X_2 \quad \text{with} \quad K_{CaX2} = [Ca\text{-}X_2]/[Ca^{2+}][X^{-}]^2 \qquad (8)$$

438 Finally, equilibrium with aragonite ($CaCO_3$) was included in the model to inspect the interaction of
439 volcanic glass ion exchange with mass transfer of the sedimentary carbonate. The modelled data for
440 Ca^{2+} compares well with the field data (Fig. 8) showing a little depletion as compared to the
441 seawater Ca/Cl ratio. In the model runs, there is very little mass transfer for aragonite with only a
442 small amount of aragonite dissolving at a low Cl and a small amount of aragonite precipitation at a
443 higher Cl concentration.

444 Mungall and Martin (1994) found that the volcanic glass surface apart from protons
445 also becomes enriched in Sr due to uptake from the solution (Cousens et al., 1993). Indeed many of
446 the volcanic groundwaters on Porto Santo, show a depletion in Sr relative to the seawater Sr/Cl ratio
447 (Fig. 3a) which is in agreement with the initial weathering of volcanic glass. The samples showing a
448 Ca/Cl ratio far above the seawater Ca/Cl ratio (Fig. 2c) are the exception. Truesdell (1966) also
449 found that volcanic glass has a preference for K^{+} over Na^{+}, which is consistent with the depletion of
450 K^{+} that is observed in many of the samples from volcanic aquifers (Fig. 3b). However, Sr^{2+} and K^{+}
451 are not quantitatively important components in Porto Santo groundwater and therefore they are not
452 included in the model. Overall, the model shows that surface exchange on the volcanic glass could
453 be a consistent explanation for the development of high $NaHCO_3$ waters. However, further work is
454 needed to verify whether the fitted exchange constants and surface site concentrations constitute
455 realistic values.

456

457 *5.3. Trace Contaminants*

458 *5.3.1. Fluoride*

459 Enhanced fluoride in groundwater is a drinking water problem affecting more than 200 million
460 people globally, and is widespread particularly in arid regions of Asia, Africa and America
461 (Edmunds and Smedley, 2013). Fluoride is dissolved in the groundwater as the free F^- ion and
462 probably has a volcanic source. During volcanic eruptions fluoride is primarily emitted in volatile
463 form. However, it may become associated with surfaces of basalts or volcanic ashes (White and
464 Hochella, 1992) or to tephra particles extracted from the hydrothermal system during steam
465 explosions (Cronin et al., 2003). In either case, fluoride forms phases such as CaF_2, MgF_2, or AlF_3,
466 on the surface of volcanic glass and these compounds may subsequently dissolve and lead to high F
467 concentrations in surface waters, which in several cases has led to the death of sheep due to
468 fluorosis (Óskarsson, 1980; Cronin, et al., 2003). Once in a surface environment fluoride can be
469 retained either in the form of fluorite, fluorapatite, become incorporated to carbonate minerals or be
470 adsorbed onto clay minerals (Du et al., 2011) and Fe-oxides (Tang et al., 2010). Fluoride is
471 preferentially incorporated in aragonite (Ichikuni, 1979; Tanaka and Ohde, 2010) as compared to
472 calcite (Kitano and Okumura, 1973). Within marine carbonate sediments, fluoride remains well
473 preserved in mineral phases like aragonite, high Mg-calcite and fluorapatite (Rude and Aller, 1991).
474 This is probably the reason why there is little difference in the F concentration between carbonate
475 and volcanic aquifers (Fig. 4a). Under the present day semi-arid groundwater conditions very little
476 flushing of fluoride out of the system will take place. The groundwater Sr concentrations above the
477 Sr/Cl seawater ratio (Fig. 3a) could indicate the dissolution of aragonite, which is able to contain a
478 high amount of fluoride. However, there is no correlation (not shown) between the Sr and F
479 concentration, suggesting that aragonite is not an important source for groundwater fluoride. As
480 shown in Fig. 5b, the distribution of the fluoride concentration is roughly inversely correlated to the
481 Ca concentration but not strictly confined to the fluorite (CaF_2) equilibrium line as has been found

in other studies (Handa, 1975). Fluoride present in the groundwater today could originate from the dissolution of fluorite, possibly mixed with waters containing less fluoride. Such mixing could occur in situ and be due to fracture flow, but may also be the result from sampling groundwater from large diameter wells, tunnels and galleries. However, fluorite has not been identified as a mineral present in the deposits.

5.3.2. Boron

As shown in Fig. 4b, almost all groundwater samples significantly exceed the WHO guideline value for boron of 0.5 mg/L (≈ 0.05 mM). Boron is suspected to have a detrimental effect on developing foetuses and testes and as a result lead to reduced fertility. High B groundwaters are reported from around the Mediterranean (Vengosh et al., 2005; Pennisi, et al., 2006; Voutsa et al., 2009), Argentina (Smedley et al., 2002), Bangladesh and the USA (Ravenscroft and McArthur, 2004). Boron is primarily present in the groundwater as boric acid (H_3BO_3) and borate ($B(OH)_4^-$). Below pH 9 most boron is present as boric acid but above pH 9 borate become the predominant form. Thus, B is present mainly as boric acid in the Porto Santo groundwater although in the samples with the highest pH, up to 50 % may be present as borate. Experimental studies indicate that boron may adsorb to clay minerals and Fe oxides. Boron may also become incorporated in carbonate minerals (Balan et al., 2016). For clay minerals and soils, the ionic strength (Goldberg et al., 1993) and the pH (Keren and Mezuman, 1981; Palmer et al., 1987) were reported to affect boron adsorption. However, in our field data there is no apparent relation between B and the EC, used as expression for the Ionic Strength (Supplementary Materials Figure A1.3) nor does pH seem to affect the B concentration (Supplementary Materials Figure A1.4). Anion competition of boron with nitrate, sulfate molybdate and phosphate on clay and soil are not important (Goldberg et al., 1996).

However, Brockamp (1973) found that the presence of bicarbonate does diminish boron adsorption on clay. Our data shows a relation between the B concentration and Alk-react, which is alkalinity corrected for the contribution derived from the seawater component and in fact B correlates even better with Na-react (Fig. 9). Ravenscroft and McArthur (2004) found similar relations in groundwater from Bangladesh and the USA. They argued that the enhanced B concentration correlated with alkalinity, indicated B release from the sediment to be due to displacement of B on surface sites by HCO_3^- as the result of aquifer freshening. This explanation could also apply to H/Na exchange on the volcanic glass surface. Interestingly, Pennisi et al. (2006) arrived to the opposite conclusion; they argue that high B in groundwater reflects groundwater intrusion and attribute the B mobilization to the ionic strength effect.

5.3.3. Arsenic

Almost 30 % of the groundwater samples from Porto Santo exceeds the WHO guideline for arsenic of 10 µg/L (≈ 0.13 µM) (Fig. 4c) and high As appears to occur more often in the carbonate than in volcanic aquifers. Arsenic in groundwater is probably globally the most serious groundwater contamination problem (Ravenscroft et al., 2009; Smedley and Kinniburgh, 2013). Arsenic contamination problems in groundwater of arid climates, have been reported from in Argentina (Nicolli et al., 1989; Bhattacharya et al., 2006; Smedley et al., 2002, 2005), Chile and Mexico and the SW USA (Smedley and Kinniburgh, 2013; Welch and Lico, 1998). Since the groundwater in these systems is oxic, dissolved arsenic will be present in the oxidized As(V) form. The groundwater on Porto Santo has a pH in the range 7.5-8.5 and the predominant species will therefore be $HAsO_4^{2-}$ (Appelo & Postma, 2005). As(V) readily adsorbed to the surfaces of Fe-oxides and clays (Martin et al., 2014) as well as on carbonate (Sø et al., 2008).

The arsenic is thought to originate mainly from volcanic glass (Nicolli et al., 1989; Bhattacharya et al., 2006; Scanlon et al., 2009) but a major part is after the release from volcanic glass retained in the sediments as adsorbed As(V). Smedley et al. (2005) and Smedley and Kinniburgh (2013) argued that desorption of As(V) towards high pH (> 8.5) is an important mobilization mechanism and Bhattacharya et al. (2006) observed a relation between dissolved As and the pH. On the other hand, Scanlon et al. (2009) found no relation between dissolved As and pH. In the Porto Santo data is there is no relation between dissolved As and pH either (Supplementary Materials Figure A1.5). Scanlon et al. (2009) argued that As mobilization could be caused by a counterion effect where the adsorption of cations changes the surface charge thereby mobilizing As.

5.3.4. Vanadium

Another solute which originates from groundwater-volcanics interactions, is vanadium which in Porto Santo groundwater reaches a concentration of up to 6 µM. Enhanced vanadium concentrations, commonly found in conjunction with fluoride and arsenic, have also been observed on the Canary island of El Hierro (Luengo-Otoz et al., 2014), near Mt Etna (Aiuppa et al., 2000; Arena et al., 2014) and Argentina (Fiorentino et al., 2007; Nicolli et al., 2012). In these oxic groundwaters vanadium will typically be present as mobile V(V) oxyanions but it has the ability to adsorb to the surfaces of particularly Fe-oxides (Wright and Belitz, 2010).

6. General assessment

The groundwater chemistry on the island of Porto Santo displays a striking similarity to what has been reported for loess deposits containing abundant volcanic glass fragments from Argentina

(Nicolli et al., 2012) and tuffaceous aquifers in the southwestern USA (White, 1979; White et al., 1980). These groundwaters are also present under arid climatic settings with little aquifer flushing. They all feature high concentrations of Na and alkalinity which are consistent with process that Na^+/H^+ exchange on the volcanic glass surface (Truesdell, 1966; White et al., 1983; Magonthier et al., 1992; Mungall and Martin, 1994) and hard to explain by any other mechanism. The Porto Santo groundwater contain a suite of minor components like F, V, As and B which previously also have been reported from the groundwaters in Argentina (Smedley et al., 2002; Nicolli et al., 2012). The presence of these trace components also indicates long groundwater residence times and little flushing of the aquifer. From a hydrogeochemical point of view, clastic deposits containing volcanic glass particles, in pyroclastic layers or embedded in loess, are much more likely as a source of volcanic glass derived ions into groundwater than basalts, because they feature a high surface area of the small glass particles as well as matrix flow while basalts predominantly have fracture flow.

7. Conclusions

1) The high $NaHCO_3$ groundwaters of the volcanic island Porto Santo are consistent with a mechanism of Na^+/H^+ exchange occurring on the volcanic glass surface. This process constitutes only the initial phase of volcanic glass alteration because it is controlled by solid state diffusion of protons into the glass and Na^+ ions out of the glass. The rate of the exchange process will therefore decrease very strongly as the exchange process moves below the glass surface.
2) An unlimited CO_2 source is needed to buffer the pH at near neutral values while building up a very high alkalinity. Unlimited CO_2 is typical present in the soil and unsaturated

groundwater zone where CO_2 is produced by respiration and organic matter oxidation and gaseous CO_2 transport is fast.

3) Arid climatic conditions with very low infiltration play an important role as well. First, they provide long groundwater residence times enabling ample time for even slow volcanic glass weathering. Second, under arid conditions only few pore volumes of groundwater will flush through the deposits retaining, apart from Na^+ and alkalinity, mobile components like fluoride, boron and vanadium in the aquifer. It follows that changing climatic conditions will strongly influence the groundwater composition with increasing concentrations when conditions become more arid and decreasing concentrations as infiltration increases.

ACKNOWLEDEMENTS

Teresa Melo and Dieke Postma dedicate this paper to the memory of our mutual friend and great hydrogeochemist the late Mike Edmunds. Special thanks to Luisa Menezes, who accompanied and helped us in finding the locations on the island during the field campaign.

REFERENCES

APA 2016. Plano Plano Regional da Água da Madeira (PRAM). https://www.apambiente.pt/?ref=16&subref=7&sub2ref=9&sub3ref=834

595 Appelo, C.A.J., 1994. Cation and proton exchange, pH variations, and carbonate reactions in a
596 freshening aquifer. Water Resour. Res. 30, 2793–2805.
597
598 Appelo C. A. J., Postma D., 2005. Geochemistry Groundwater and Pollution, 2nd ed.
599 Balkema Publ. 649 pp.
600
601 Aiuppa, A., Allard, P., D'Alessandro, W., Michel, A., Parello, F., Treuil, M., Valenza, M., 2000.
602 Mobility and fluxes of major, minor and trace metals during basalt weathering and groundwater
603 transport at Mt. Etna volcano (Sicily). Geochimica Cosmochimica Acta 64 (11), 1827–1841.
604
605 Arena, G., Copat, C., Dimartino, A., Grasso, A., Fallico, R., Sciacca, S., Fiore, M., Ferrante, M.,
606 2014. Determination of total vanadium and vanadium(V) in groundwater from Mt. Etna and
607 estimate of daily intake of vanadium(V) through drinking water. J. Water Health 13 (2), 522-530.
608 https://doi.org/10.2166/wh.2014.209
609
610 Balan, E., Pietrucci, F., Gervais, C., Blanchard, M., Schott, J., Gaillardet, J., 2016, First-principles
611 study of boron speciation in calcite and aragonite, Geochimica Cosmochimica Acta 193, 119–131.
612
613 Bhattacharya, P., Claesson, M., Bundschuh, J., Sracek, O., Fagerberg, J., Jacks, G., Martin, R.A.,
614 Storniolo, A.D., Thir, J.M., 2006, Distribution and mobility of arsenic in the Rio Dulce alluvial
615 aquifers in Santiago del Estero Province, Argentina. Sci. Total. Environ. 358, 97–120.
616
617 Brockamp, O., 1973. Borfixierung in authigenen und detritischen Tonen. Geochimica
618 Cosmochimica Acta 37, 1339-1351.

Burke, K., Wilson, J. T., 1972. Is the African plate stationary? Nature 239, 387–90.

Carracedo, J. C., 1999. Growth, structure, instability and collapse of Canarian volcanoes and comparisons with Hawaiian volcanoes. J. Volcanol. Geotherm. Res. 94,1–19.

Carreira, P. M., Marques, J. M., Pina, A., Gomes, A. M., Fernandes, P. A. G.,· Santos, F. M., 2010. Groundwater Assessment at Santiago Island (Cabo Verde): A Multidisciplinary Approach to a Recurring Source of Water Supply. Water Resour. Management 24, 1139–1159. DOI 10.1007/s11269-009-9489-z

Condesso de Melo, M.T., 2002. Flow and hydrogeochemical mass transport model of the Aveiro Cretaceous multilayer aquifer (Portugal). PhD thesis, Universidade de Aveiro, Portugal. https://ria.ua.pt/bitstream/10773/2753/1/2009001201.pdf

Condesso de Melo, M. T., Silva, J. Lobo de Pina, A., Mota Gomes, A., Almeida, F., Moura, R., Marques da Silva, M. A., 2008. Use of Geochemical Tools to Study Groundwater Salinization in Volcanic Islands: a Case Study in the Porto Santo (Portugal) and Santiago (Cape Verde) Islands 20th Salt Water Intrusion Meeting June 23-27, Naples, Florida, USA pp. 41-44.

Cousens, B. L., Spera, F. J., Dobson, P. F., 1993. Post-eruptive alteration of silicic ignimbrites and lavas, Gran Canaria, Canary Islands: Strontium, neodymium, lead, and oxygen isotopic evidence. Geochimica Cosmochimica Acta 57,631-640.

643 Cronin, S. J., Neall, V. E., Lecointre, J.A., Hedley, M.J., Loganathan, P., 2003. Environmental
644 hazards of fluoride in volcanic ash: a case study from Ruapehu volcano, New Zealand. J. Volcanol.
645 Geotherm. Res. 121, 271-291.
646
647 Cropper, T. 2013. The weather and climate of Macaronesia: past, present and future. Weather 68,
648 No. 11, 300-307.
649
650 Cropper, T. E., Hanna, E., 2014. An analysis of the climate of Macaronesia, 1865–2012. Int. J.
651 Climatol. 34, 604–622.
652
653 Crovisier, J.L., Honnorez, J., Fritz, B., 1992. Dissolution of subglacial volcanic glasses from
654 Iceland: laboratory study and modelling. Applied Geochemistry. Suppl. Issue No. 1. pp. 55-81.
655
656 Cruz, J. V., Fontiela, J. Prada, S., Andrade, C. 2014, The chemical status of groundwater and
657 pollution risk in the Azores archipelago (Portugal) Environ. Earth Sci. DOI 10.1007/s12665-014-
658 3407-2
659
660 Custodio, E., del Carmen Cabrera, M., Poncela, R., Puga, L-O., Skupien, E., del Villar, A., 2016.
661 Groundwater intensive exploitation and mining in Gran Canaria and Tenerife, Canary Islands,
662 Spain: Hydrogeological, environmental, economic and social aspects. Sci. Total. Environ. 557–558,
663 425–437. http://dx.doi.org/10.1016/j.scitotenv.2016.03.038
664

665 Du, J., Wu, D., Xiao, H., Li, P., 2011, Adsorption of fluoride on clay minerals and their
666 mechanisms using X-ray photoelectron spectroscopy. Front. Environ. Sci. Engin. China 5, (2), 212–
667 226.
668
669 Dubroeucq, D., Geissert, D., Quantin, P., 1998. Weathering and soil forming processes under semi-
670 arid conditions in two Mexican volcanic ash soils. Geoderma 86, 99-122.
671
672 Edmunds, W. M., Smedley, P. L., 2013,.Fluoride in natural waters. In O.Selenius et al. (Eds)
673 Essentials of Medical Geology, Revised Edition. British Geological Survey 311-336.
674
675 European Community, 1998. Council directive 98/83 Official Journal of the European Community.
676
677 Ferreira, M., Portugal, M., Macedo, C. R., Ferreira, J. F., 1988. K-Ar geocronology in the
678 Selvagens, Porto Santo and Madeira islands (Eastern Central Atlantic): A 30 my spectrum of
679 submarine and subaerial volcanism. Lunar Plant. Inst., 19, pp. 325-326.
680
681 Ferreira, M. R. P. V., Neiva, J. M. C., 1996. Carta geológica de Portugal: Folha da lha de Porto
682 Santo, Centro de Geociências da Universidade de Coimbra, Instituto Geológico e Mineiro, Lisboa.
683
684 Fiore, S., Huertas, F. J., Tazaki, K., Huertas, F., Linares J., 1999. A low temperature experimental
685 alteration of a rhyolitic obsidian. Eur. J. Mineral. 11, 455–469.
686

687 Fiorentino, C. E., Paoloni, J. D., Sequeira, M. E., Arosteguy, P., 2007. The presence of vanadium in
688 groundwater of southeastern extreme the pampean region Argentina: Relationship with other
689 chemical elements. J. Contam. Hydrol. 93, (1–4), 122–129.
690
691 Flaathen, T. K., Gislason, S. R., Oelkers, E. H., Sveinbjörnsdóttir, Á. E., 2009. Chemical evolution
692 of the Mt. Hekla, Iceland, groundwaters: A natural analogue for CO_2 sequestration in basaltic rocks.
693 Appl. Geochem. 24, 463-474.
694
695 Geldmacher, J., Hoernle, K., v. d. Bogaard, P., Zankl, G., Garbe-Schönberg, D., 2001. Earlier
696 history of the 70-Ma-old Canary hotspot based on the temporal and geochemical evolution of the
697 Selvagen archipelago and neighboring seamounts in the eastern North Atlantic, J. Volcanol.
698 Geotherm. Res.,111, 55– 87.
699
700 Geldmacher, J., Hoernle, K., Klügel, A., v. d. Bogaard, P., Wombacher, F., Berning, B., 2006.
701 Origin and geochemical evolution of the Madeira-Tore Rise (eastern North Atlantic). J.
702 Geophysical Res. 111, B09206, doi:10.1029/2005JB003931, 2006
703
704 Gislason, S. R., Eugster, H. P., 1987. Meteoric water-basalt interactions: II. A field study in NE
705 Iceland Geochimica Cosmochimica Acta 51**,** 2841–2855.
706
707 Gislason, S.R., Oelkers, E.H., 2003. Mechanism, rates, and consequences of basaltic glass
708 dissolution: II. An experimental study of the dissolution rates of basaltic glass as a function of pH
709 and temperature. Geochim. Cosmochim. Acta 67, 3817-3832.
710

711 Goldberg, S., Forster, H. S., Heick, E. L., 1993. Boron adsorption mechanisms on metal oxides,
712 clay-minerals, and soils inferred from ionic-strength effects. Soil Sci. Soc. Am. J. 57, 704–708.
713
714 Goldberg, S., Forster, H. S., Lesch, S. M., Heick, E. L., 1996. Influence of anion competition on
715 boron adsorption by clays and soils. Soil Sci. 161, 99–103.
716
717 Handa, B. K., 1975. Geochemistry and genesis of fluoride-containing ground waters in India.
718 Ground Water 13, 275–281.
719
720 Heilweil, V. M., Earle, J. D., Cederberg, J. R., Messer, M. M., Jorgensen, B. E., Verstraeten, I. M.,
721 Moura, M. A., Querido, A., Spencer, F., Osorio, T., 2006. Evaluation of baseline ground-water
722 conditions in the Mosteiros, Ribeira Paúl, and Ribeira Fajã Basins, Republic of Cape Verde, West
723 Africa, 2005–06: U.S. Geological Survey Scientific Investigations Report 2006-5207, 42 p.
724
725 Heilweil, V. M., Solomon, D. K., Gingerich, S. B., Verstraeten, I. M., 2009. Oxygen, hydrogen, and
726 helium isotopes for investigating groundwater systems of the Cape Verde Islands, West Africa:
727 Hydrogeology J. 17 (5), 1157-1174.
728
729 Heilweil, V. M., Healy, R. W., Harris, R. N., 2012. Noble gases and coupled heat/fluid flow
730 modeling for evaluating hydrogeologic conditions of volcanic island aquifers**.** J. Hydrology
731 464–465, 309-327. doi.org/10.1016/j.jhydrol.2012.07.019
732

733 Herrera, C., Custodio, E., 2014. Groundwater flow in a relatively old oceanic volcanic island: The
734 Betancuria area, Fuerteventura Island, Canary Islands, Spain. Sci. Total. Environ. 496, 531–550.
735 http://dx.doi.org/10.1016/j.scitotenv.2014.07.063
736
737 Holik, J. S., Rabinowitz, P. D., Austin, J. A., 1991. Effects of the Canary hotspot volcanism on
738 structure of oceanic crust off Morocco. J. Geophys. Res. 96, 12,039– 12,067.
739
740 Ichikuni, M., 1979. Uptake of fluoride by aragonite. Chem. Geol. 27, 207-214.
741
742 IPMA 2017. Tempo. Rede de Estações de Superfície. Porto Santo. https://www.ipma.pt/
743
744 Keren, R., Mezuman, V., 1981. Boron adsorption by clay minerals using a phenomenological
745 equation. Clays Clay Minerals 29, 198-204.
746
747 Kitano, Y., Okumura, M., 1973. Coprecipitation of fluoride with calcium carbonate. Geochem. J. 7,
748 37-49.
749
750 Luengo-Otoz, N., Bellomo, S., D'Alessandro, W., 2014. High vanadium concentrations in
751 groundwater at El Hierro (Canary Islands, Spain) 10th International Hydrogeological Congress of
752 Greece / Thessaloniki, 427-435.
753

754 Lutze, W., Malow, G., Ewing, R. C., Jercinovic M. J., Keil, K., 1985. Alteration of basalt glasses:
755 implications for modeling the longterm stability of nuclear waste glasses. Nature 314**,** 252–255.
756
757 Magonthier, M., Petit, J., Dran, J., 1992. Rhyolitic glasses as natural analogues of nuclear waste
758 glasses: Behaviour of an Icelandic glass upon natural aqueous corrosion. Appl. Geochem.Supp. 1,
759 83–93.
760
761 Martin, M., Violante, A., Ajmone-Marsan, F., Barberis, E., 2014. Surface Interactions of Arsenite
762 and Arsenate on Soil Colloids. Soil. Sci. Soc. Am. J. 78, 157-170.
763
764 Mata, J., Kerrich, R., MacRae, N. D., Wu, T. W., 1998. Elemental and isotopic (Sr, Nd, and Pb)
765 characteristics of Madeira Island basalts: evidence for a composite HIMU-EM I plume fertilizing
766 lithosphere. Canadian Journal of Earth Sciences, 35(9), 980-997.
767
768 Matter, J. M., Stute, M., Snæbjörnsdóttir, S. Ó., Oelkers, E. H., Gislason, S. R., Aradottir, E. S.,
769 Sigfusson, B., Gunnarsson, I., Sigurdardottir, H., Gunnlaugsson, E., Axelsson, G., Alfredsson,
770 H. A., Wolff-Boenisch, D., Mesfin, K., Fernandez de la Reguera Taya, D., Hall, J., Dideriksen, K.,
771 Broecker, W. S., 2016. Rapid carbon mineralization for permanent and safe disposal of
772 anthropogenic carbon dioxide emissions. Science 352, 1312-1314.
773
774 Mendes, S., 2006. Fluorose e cárie dentária na Ilha de Porto Santo: um estudo epidemiológico.
775 MSc Thesis. Universidade de Lisboa. Lisboa.
776

Mirabella, A., Egli, M., Raimondi, S., Giacca, D., 2005. Origin of clay minerals in soils on pyroclastic deposits in the island of Lipari (Italy). Clays and Clay Min. 53, 409-421.

Mungall, J. E., Martin, R. F., 1994. Severe leaching of trachyte glass without devitrification, Terceira, Azores. Geochim. Cosmochim. Acta 58, 75–83.

Nicolli, H. B., Suriano, J. M., Peral, M. A. G., Ferpozzi, L. H., Baleani, O. A., 1989. Groundwater contamination with arsenic and other trace-elements in an area of the Pampa, province of Cordoba, Argentina. Environ. Geol. Water Sci. 14, 3–16.

Nicolli, H. B., García, J. W., Falcón, C. M., Smedley, P. L., 2012. Mobilization of arsenic and other trace elements of health concern in groundwater from the Salí River Basin, Tucumán Province, Argentina. Environ. Geochem. Health 34, 251–262.

Óskarsson, N., 1980. The interaction between volcanic gasses and tephra: fluorine adhering to tephra of the 1970 Hekla eruption. J. Volcanol. Geotherm. Res. 8, 251-266.

Palmer, M. R., Spivack, A. J., Edmond, J. M., 1987, Temperature and pH controls over isotopic fractionation during adsorption of boron on marine clay. Geochimica Cosmochimica Acta 51, 2319-2323.

Parkhurst, D. L., Appelo, C. A. J., 2013. Description of input and examples for PHREEQC version 3—A computer program for speciation, batch-reaction, one-dimensional transport, and

inverse geochemical calculations: U.S. Geological Survey Techniques and Methods, 2013, book 6, chap. A43, 497 p., available only at <http://pubs.usgs.gov/tm/06/a43>.

Patriat, M., Labails, C., 2006. Linking the Canary and Cape-Verde hot-spots, Northwest Africa. Mar. Geophys. Res. 27, 201–15.

Penman, H. L., 1948. Natural evaporation from open water, bare soil and grass. Proceedings of the Royal Society of London, Series A 193, p. 120–145.

Pennisi, M., Bianchini, G., Muti, A., Kloppmann, W., Gonfiantini, R., 2006. Behaviour of boron and strontium isotopes in groundwater-aquifer interactions in the Cornia Plain (Tuscany, Italy), Appl. Geochem. 21 (2006) 1169–1183.

Postma, D., Kjøller, C., Andersen, M. S., Condesso de Melo, M. T., Gaus, I. 2009. Geochemical Modelling of Processes Controlling Baseline Compositions of Groundwater. in W.M. Edmunds & P. Shand (Eds.) Natural Groundwater Quality. Wiley. https://doi.org/10.1002/9781444300345.ch4

Prada, S., Silva, M.O., Cruz, J.V., 2005. Groundwater behaviour in Madeira, volcanic island (Portugal). Hydrogeol. J. 13, 800–812. http://dx.doi.org/10.1007/s10040-005-0448-3.

Ravenscroft, P., McArthur, J.M., 2004, Mechanism of regional enrichment of groundwater by boron: the examples of Bangladesh and Michigan, USA. Appl. Geochem. 19, 1413–1430.

825 Ravenscroft, P., Brammer, H., Richards K., 2009 Arsenic Pollution: A Global Synthesis, Wiley-
826 Blackwell.
827
828 Ribeiro, M.L., Ramalho, M., 2010. A Geological tour of the islands of Madeira and Porto Santo.
829 Direcção Regional do Comércio, Indústria e Energia. Laboratório Nacional de Energia e Geologia,
830 I.P. ISBN: 978-989-675-008-4. Lisbon.
831
832 Rude, P. D., Aller, R. C., 1991. Fluorine mobility during early diagenesis of carbonate sediment:
833 An indicator of mineral transformations. Geochimica Cosmochimica Acta 55, 2491-2509.
834
835 Scanlon, B. R., Nicot, J.P., Reedy, R.C., Kurtzman, D., Mukherjee, A., Nordstrom, D.K. 2009.
836 Elevated naturally occurring arsenic in a semiarid oxidizing system, Southern High Plains aquifer,
837 Texas, USA. Appl. Geochem. 24, 2061–2071.
838
839 SCH, 2001. Superior Council of Health, Italian Ministery of Health, Sessione XLIII, Sezione III.
840 Seduta del 18 gennaio 1995 su DPR. 236/88. Caratteristiche di qualit. delle acque destinate al
841 consumo umano. Eventuale fissazione della CMA al parametro 54-vanadio. Gazzetta Ufficiale
842 (Suppl. Ord.) n.52, 3 marzo 2001.
843
844 Shandilya, R. N., 2017. Origin of natural occurring groundwater salinity and hydrogeochemical
845 processes in the island of Porto Santo (Portugal). M.Sc. Thesis, Instituto Superior Técnico,
846 Universidade de Lisboa, Portugal. 87 pp.
847 https://fenix.tecnico.ulisboa.pt/downloadFile/1970719973966552/Raghwendra%20MSc%20Exami
848 nation%20Version.pdf

Silva, J. B. P., 2002. Beach sand of the island of Porto Santo: geology, genesis, dynamics and medicinal properties, Doctoral Dissertation in Geology. Aveiro: University of Aveiro.

Silva, J. B. P. et al., 2008. Estudo hidrogeológico da caracterização e classificação da água subterrânea do Conjunto Turístico Colombo`s Resort, ilha, Funchal: s.n.

Smedley, P. L., Nicolli, H. B., Macdonald, D. M. J., Barros, A. J., Tullio, J. O. 2002. Hydrogeochemistry of arsenic and other inorganic constituents in groundwaters from La Pampa, Argentina. Appl. Geochem. 17, 259–284.

Smedley, P. L., Kinniburgh, D. G., Macdonald, D. M. J., Nicolli, H. B., Barros, A. J., Tullio, J. O., Pearce, J. M., Alonso, M. S., 2005. Arsenic associations in sediments from the loess aquifer of La Pampa, Argentina. Appl. Geochem. 20, 989–1016.

Smedley, P. L. Kinniburgh, D. G., 2013. Arsenic in Groundwater and the Environment. in O. Selinus et al. (eds.), Essentials of Medical Geology: Revised Edition, DOI 10.1007/978-94-007-4375-5_12, British Geological Survey. Pp. 279-310.

Snæbjörnsdóttir, S. Ó., Oelkers, E. H., Mesfin, K., Aradóttir, E. S., Dideriksen, K., Gunnarsson, I., Gunnlaugsson, E., Matter, J. M., Stute, M. and Gislason, S. R., 2017. The chemistry and saturation states of subsurface fluids during the in situ mineralisation of CO_2 and H_2S at the CarbFix site in SW-Iceland. Int. J. Greenh. Gas Control 58, 87-102.

873 Snæbjörnsdóttir, S. Ó., Gislason, S. R., Galeczka, I. M., Oelkers, E. H., 2018. Reaction path
874 modelling of *in-situ* mineralisation of CO2 at the CarbFix site at Hellisheidi, SW-Iceland.
875 Geochimica Cosmochimica Acta 220, 348-366.
876
877 Stuyfzand, P. J., 1993. Hydrochemistry and hydrology of the coastal dune area of the Western
878 Netherlands. Ph.D. Thesis, Free University, Amsterdam, 366 pp.
879
880 Sø, H. U., Postma, D., Jakobsen, R., Larsen, F., 2008. Sorption and desorption of arsenate and
881 arsenite on calcite. Geochim Cosmochim Acta 72, 5871–5884.
882
883 Tanaka, K., Ohde, S., 2010. Fluoride in coral aragonite related to seawater carbonate. Geochem. J.
884 44, 371-378.
885
886 Tang, Y., Wang, J., Gao, N., 2010. Characteristics and model studies for fluoride and arsenic
887 adsorption on goethite. J. Environ. Sci., 22 (11), 1689–1694.
888
889 Thornthwaite, C. W., 1948. An approach toward a rational classification of climate. Geographical
890 review 38 (1), 55-94.
891
892 Truesdell, A. H., 1966. Ion-exchange constants of natural glasses by the electrode method. Amer.
893 Mineral. 51, 110-122.
894

Turekian, K. K., 1968. *Oceans*. Prentice-Hall, 120 pp.

Vengosh, A., Kloppmann, W., Marei, A., Livshitz, Y., Gutierrez, A., Banna, M., Guerrot, C., Pankratov, I., Raanan, H., 2005. Sources of salinity and boron in the Gaza strip: natural contamination flow in the southern Mediterranean coastal aquifer. Wat. Resour. Res. 41, W01013.

Vernaz, E. Y., Dussossoy, J. L., 1992. Current state of knowledge of nuclear waste glass corrosion mechanisms: The case of R7T7 glass. Appl. Geochem. 1. 13-22 (suppl.)

Voutsa, D., Dotsikab, E., Kourasa, A., Poutoukis, D., Kouimtzis, Th., 2009. Study on distribution and origin of boron in groundwater in the area of Chalkidiki, Northern Greece by employing chemical and isotopic tracers. J. Hazardous Materials 172, 1264–1272.

Walraevens, K. and Cardenal, J., 1994. Aquifer recharge and exchangeable cations in a Tertiary clay layer (Bartonian clay, Flanders-Belgium). Min. Mag. 58A, 955–956.

Welch, A. H., Lico, M. S., 1998. Factors controlling As and U in shallow ground water, southern Carson Desert, Nevada. Appl. Geochem. 13, 521-539.

White, A. F., 1979. Geochemistry of ground water associated with tuffaceous rocks, Oasis Valley, Nevada. U.S. Geol. Surv. Prof. Paper 712-E, 1-25

White A. F., 1983. Surface chemistry and dissolution kinetics of glassy rocks at 25°C. Geochimica Cosmochimica Acta 47, 805–815.

White, A. F., Hochella Jr., M. F., 1992. Surface chemistry associated with the cooling and subaerial weathering of recent basalt flows. Geochimica Cosmochimica Acta 56, 3711 – 3721.

White A. F, Claassen H. C, Benson L. V., 1980. The effect of dissolution of volcanic glass on the water chemistry in a tuffaceous aquifer, Rainier Mesa, Nevada. U. S. G. S. Water Supply Paper. 1535-Q.

Wolff-Boenisch, D., Gislason, S. R., Oelkers, E. H., Putnis, C. V., 2004. The dissolution rates of natural glasses as a function of their composition at pH 4 and 10.6, and temperatures from 25 to 74°C. Geochimica Cosmochimica Acta 68, 4843-4858.

Wright, M. T., Belitz, K., 2010. Factors controlling the regional distribution of Vanadium in groundwater. Ground Water 48, 515-525.

934 **FIGURE CAPTIONS**

935 Fig. 1. Main hydrogeological units of Porto Santo island (modified from Ferreira & Neiva, 1996).
936 Groundwater sampling sites are indicated with dots.

937

938 Fig. 2. Bulk water chemistry as related to aquifer rock. The sea-line reflects the ion/Cl ratio in
939 seawater. Also indicated are the recommended maximum concentrations in drinking water by the
940 WHO.

941

942 Fig. 3. Water chemistry in carbonate (blue) and volcanic (red) aquifer rock. A detailed symbol
943 lithology legend is given in Fig. 2c. The sea-line reflects the ion/Cl ratio in seawater. Also indicated
944 are the recommended maximum concentrations in drinking water
945 by the WHO.

946

947 Fig. 4. Trace components in groundwater from carbonate (blue) and volcanic (red) aquifers. A
948 detailed symbol lithology legend is given in Fig. 2c. The sea-line reflects the ion/Cl ratio in
949 seawater. Also indicated are the recommended maximum concentrations in drinking water by the
950 WHO.

951

952 Fig. 5. The saturation state of the groundwater versus a) $CaCO_3$, calcite and aragonite, and b) CaF_2,
953 fluorite. Ion activities calculated with PHREEQC are compared with solubility products given by

954 the lines. Blue indicate carbonate aquifer and red volcanic aquifer with a detailed symbol lithology
955 legend presented in Fig. 2c.

956

957 Fig. 6. The saturation state of the groundwater versus different forms of SiO_2. Blue indicate
958 carbonate aquifer and red volcanic aquifer with a detailed symbol lithology legend presented in Fig.
959 2c.

960

961 Fig. 7. Groundwater chemistry compared with a modelled freshening scenario as explained in the
962 main text. Blue dotted lines reflect the PHREEQC model predictions. Solid black lines indicate the
963 ion/Cl ratio in seawater.

964

965 Fig. 8. Groundwater chemistry as compared to the Na/Cl volcanic glass exchange PHREEQC
966 model for three different surface site concentrations with different fitted exchange constants as
967 given in Table 1. Black solid lines indicate the ion/Cl ratio in seawater.

968

969 Fig. 9. Boron in groundwater versus the concentrations of Na and alkalinity corrected for their
970 seawater contribution. The seawater contribution is calculated from the ion/Cl ratio in seawater
971 multiplied with the Cl concentration in the groundwater. Blue indicate carbonate aquifer and red
972 volcanic aquifer with a detailed symbol lithology legend presented in Fig. 2c.

973

974

975

976

977

978 Table 1. Parameters used in the PHREEQC model for volcanic glass exchanger, to fit the

979 groundwater composition in Fig. 8.

exchange site conc. X^- mol/L	log $K_{H\text{-}X}$	log $K_{Mg\text{-}X2}$	surface Na-X displaced mole %
1	4.5	-2.3	0.5-1.5
0.1	5.6	-1.3	5.8-15.5
0.05	6.0	-1.0	12-31

980

981

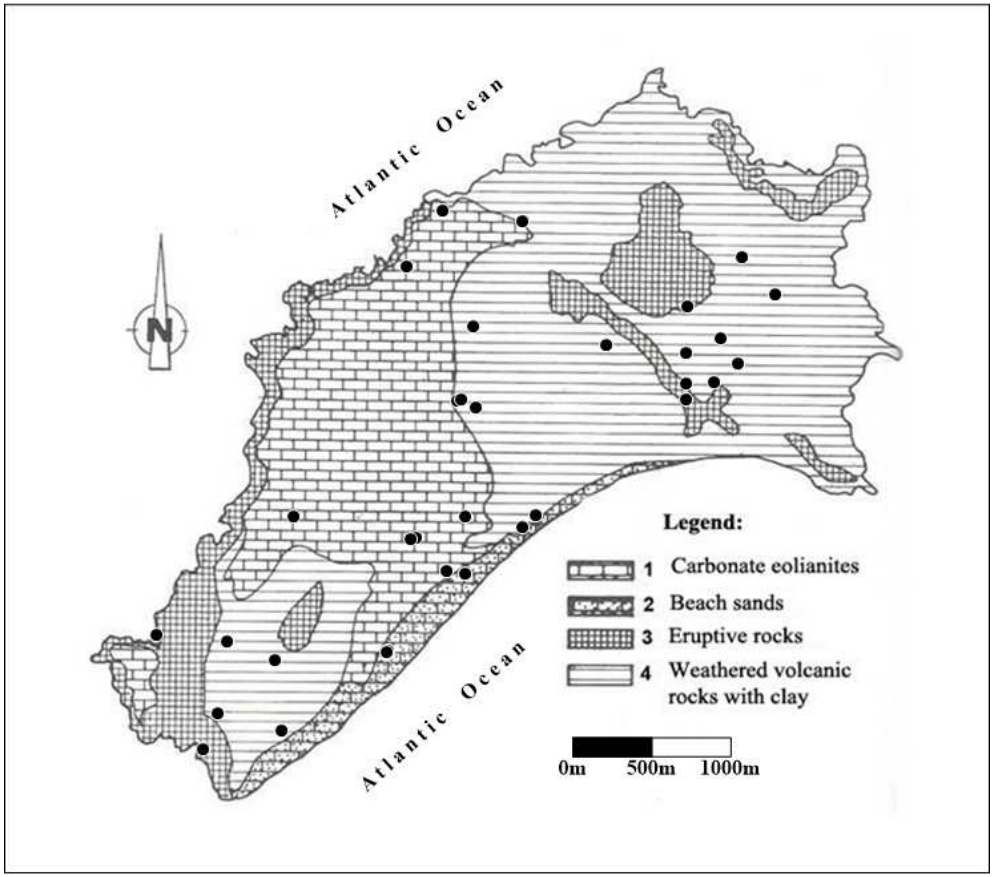

Fig. 1. Main hydrogeological units of Porto Santo island (modified from Ferreira and Neiva, 1996). Groundwater sampling sites are indicated with dots.

Porto Santo data_dieke_v4R.xlsx

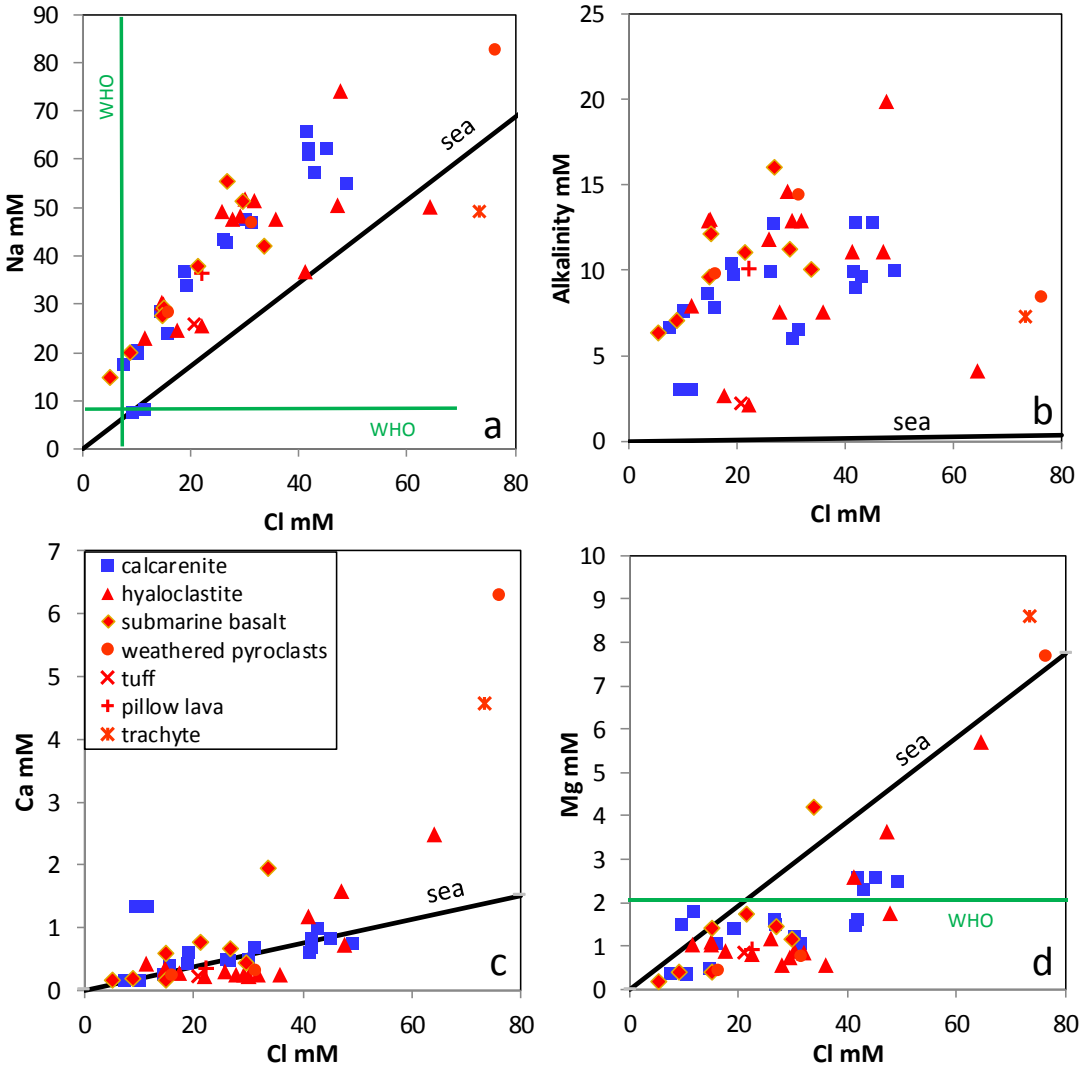

Fig. 2. Bulk water chemistry as related to aquifer rock. The sea-line reflects the ion/Cl ratio in seawater. Also indicated are the recommended maximum concentrations in drinking water by the WHO.

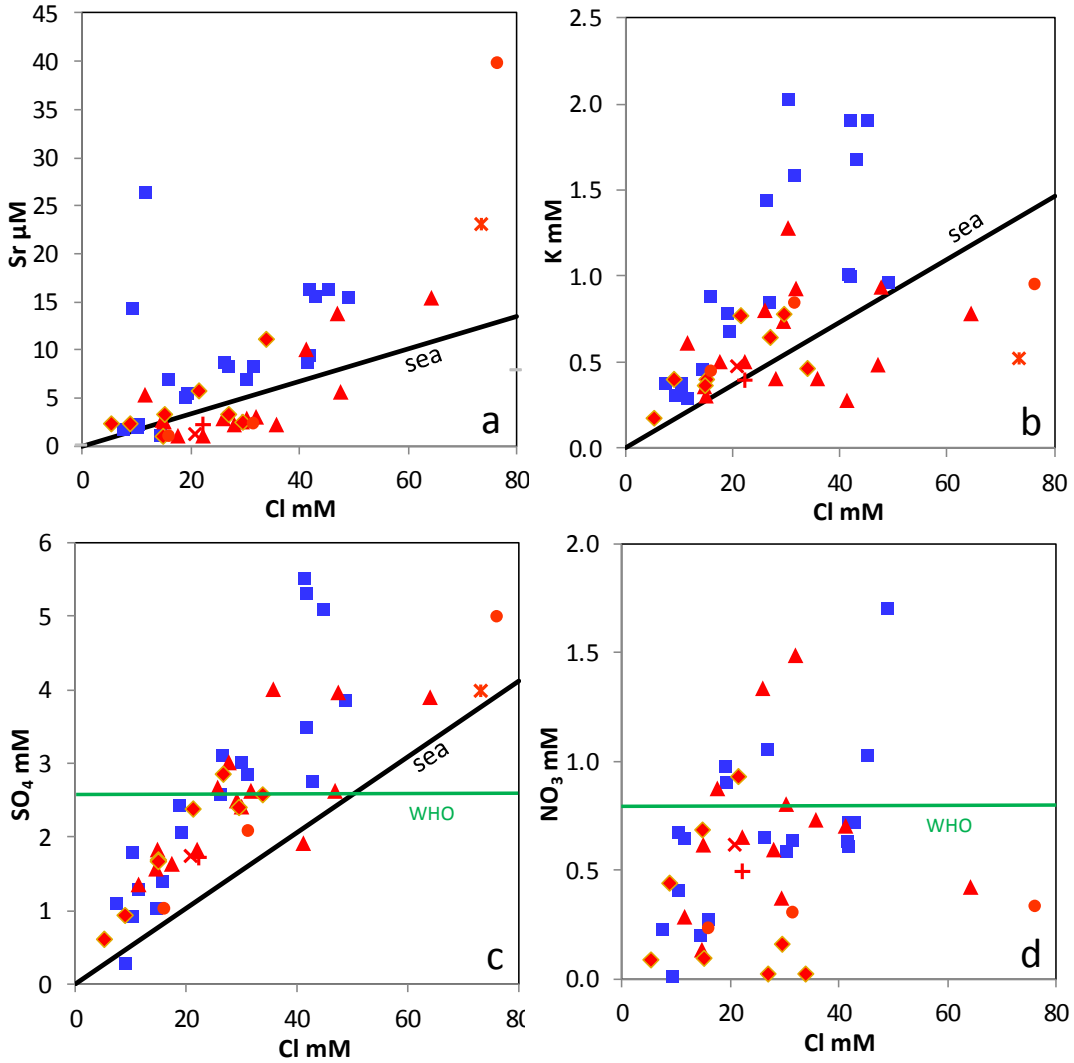

Porto Santo data_dieke_v4R.xlsx

Fig. 3. Water chemistry in carbonate (blue) and volcanic (red) aquifer rock. A detailed symbol lithology legend is given in Fig. 2c. The sea-line reflects the ion/Cl ratio in seawater. Also indicated are the recommended maximum concentrations in drinking water by the WHO.

Porto Santo data_dieke_v4R.xlsx

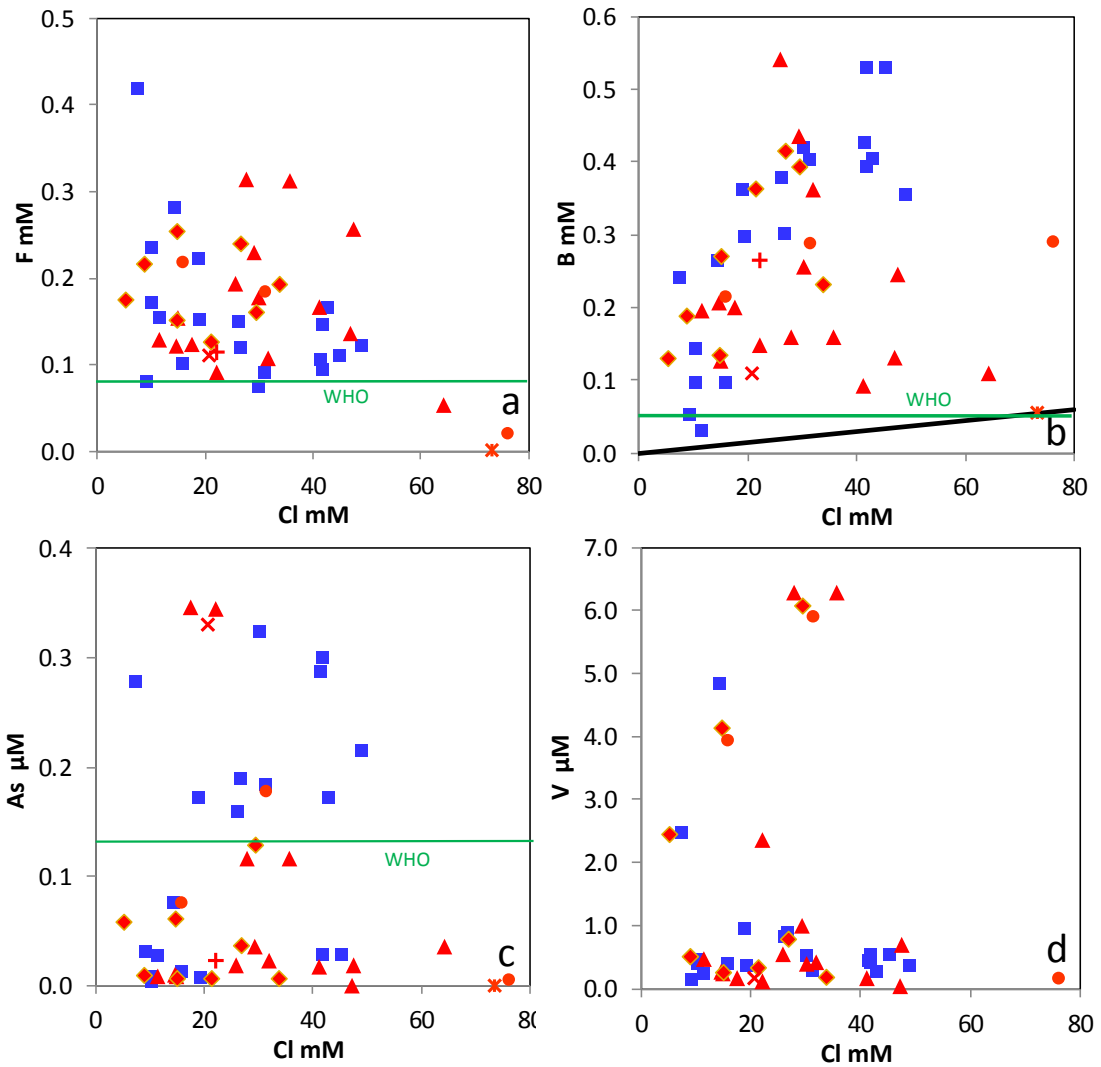

Fig. 4. Trace components in groundwater from carbonate (blue) and volcanic (red) aquifers. A detailed symbol lithology legend is given in Fig. 2c. The sea-line reflects the ion/Cl ratio in seawater. Also indicated are the recommended maximum concentrations in drinking water by the WHO.

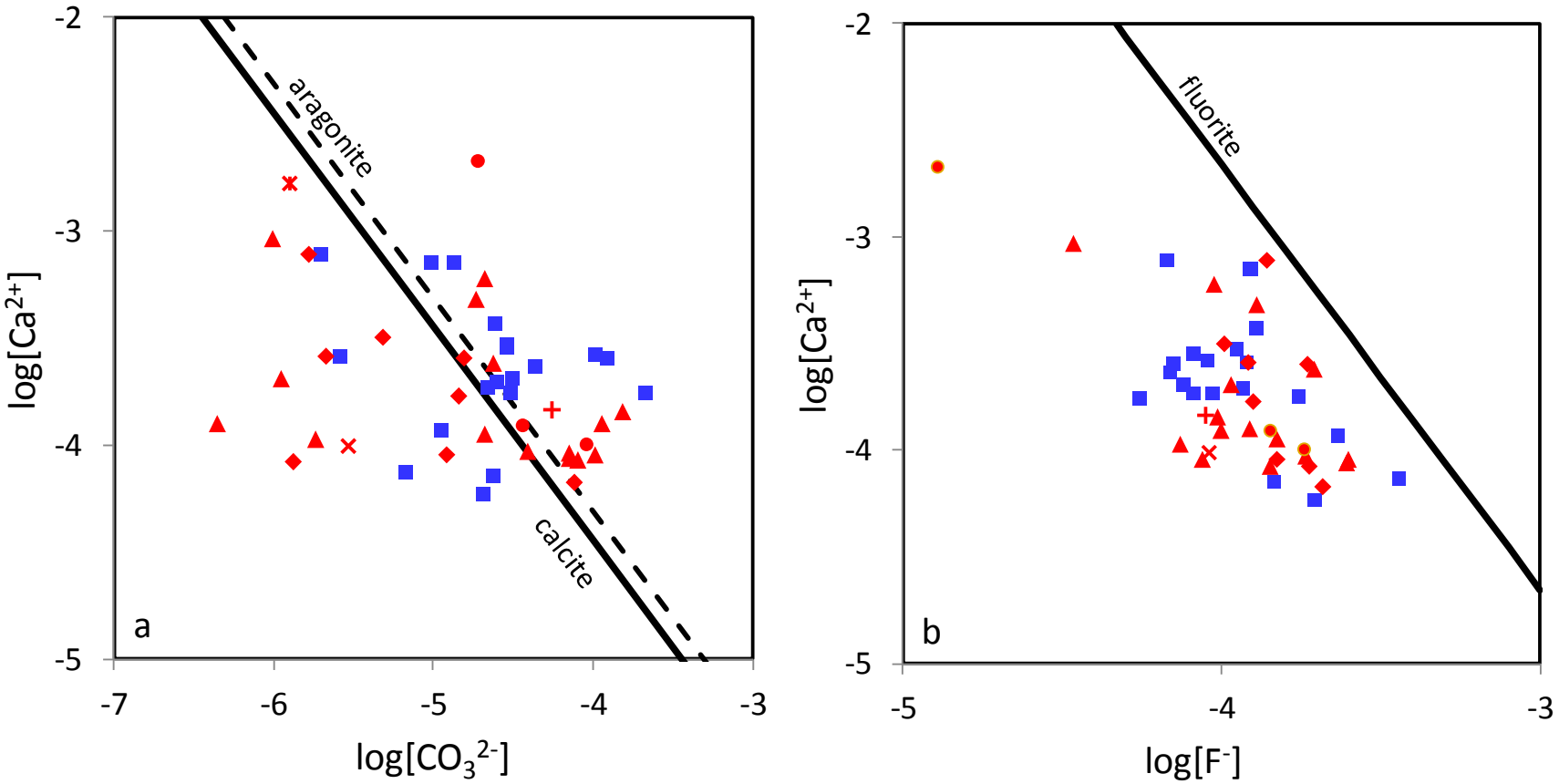

Fig. 5. The saturation state of the groundwater versus a) $CaCO_3$, calcite and aragonite, and b) CaF_2, fluorite. Ion activities calculated with PHREEQC are compared with solubility products given by the lines. Blue indicate carbonate aquifer and red volcanic aquifer with a detailed symbol lithology legend presented in Fig. 2c.

Porto Santo data_dieke_v4R.xlsx

Porto Santo data_dieke_v4R.xlsx

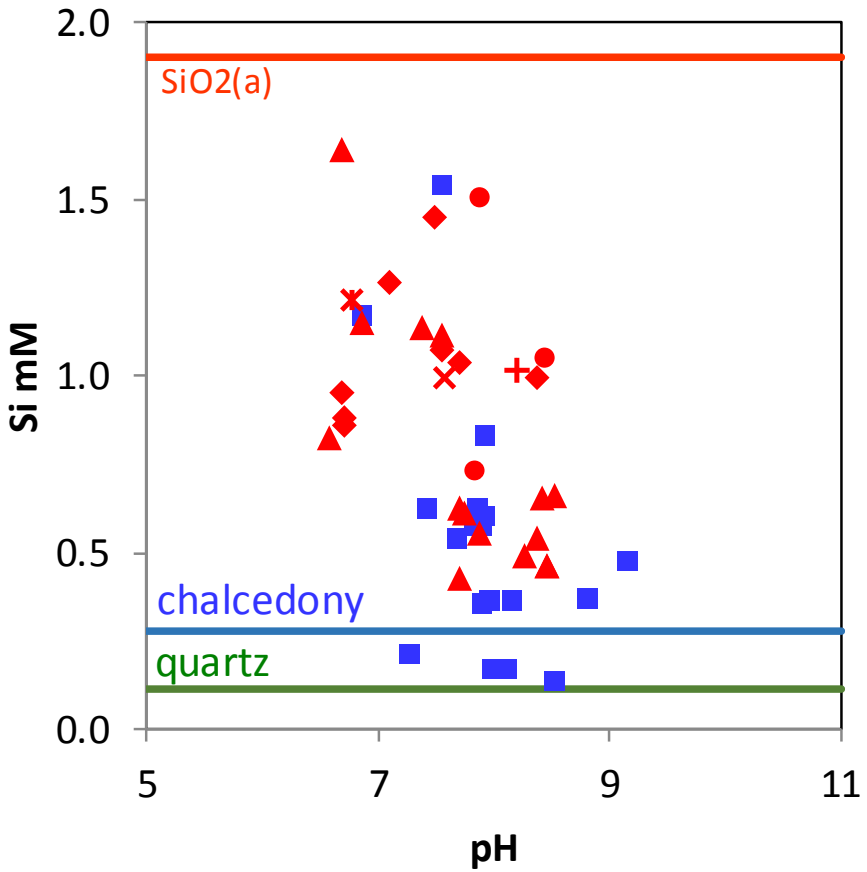

Fig. 6. The saturation state of the groundwater versus different forms of SiO_2. Blue indicate carbonate aquifer and red volcanic aquifer with a detailed symbol lithology legend presented in Fig. 2c.

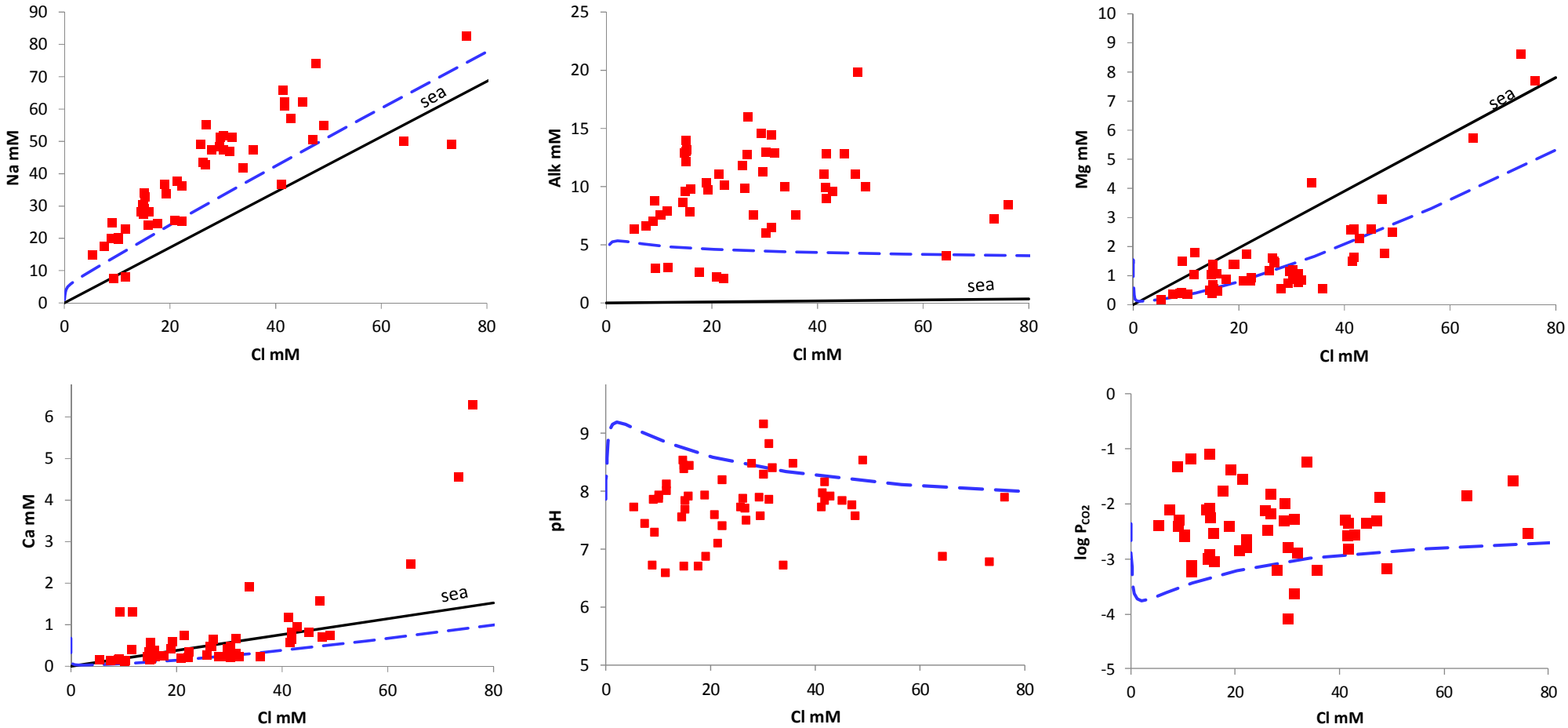

Fig. 7. Groundwater chemistry compared with a modelled freshening scenario as explained in the main text. Blue dotted lines reflect the PHREEQC model predictions. Solid black lines indicate the ion/Cl ratio in seawater.

Porto Santo data_dieke_v2.xlsx

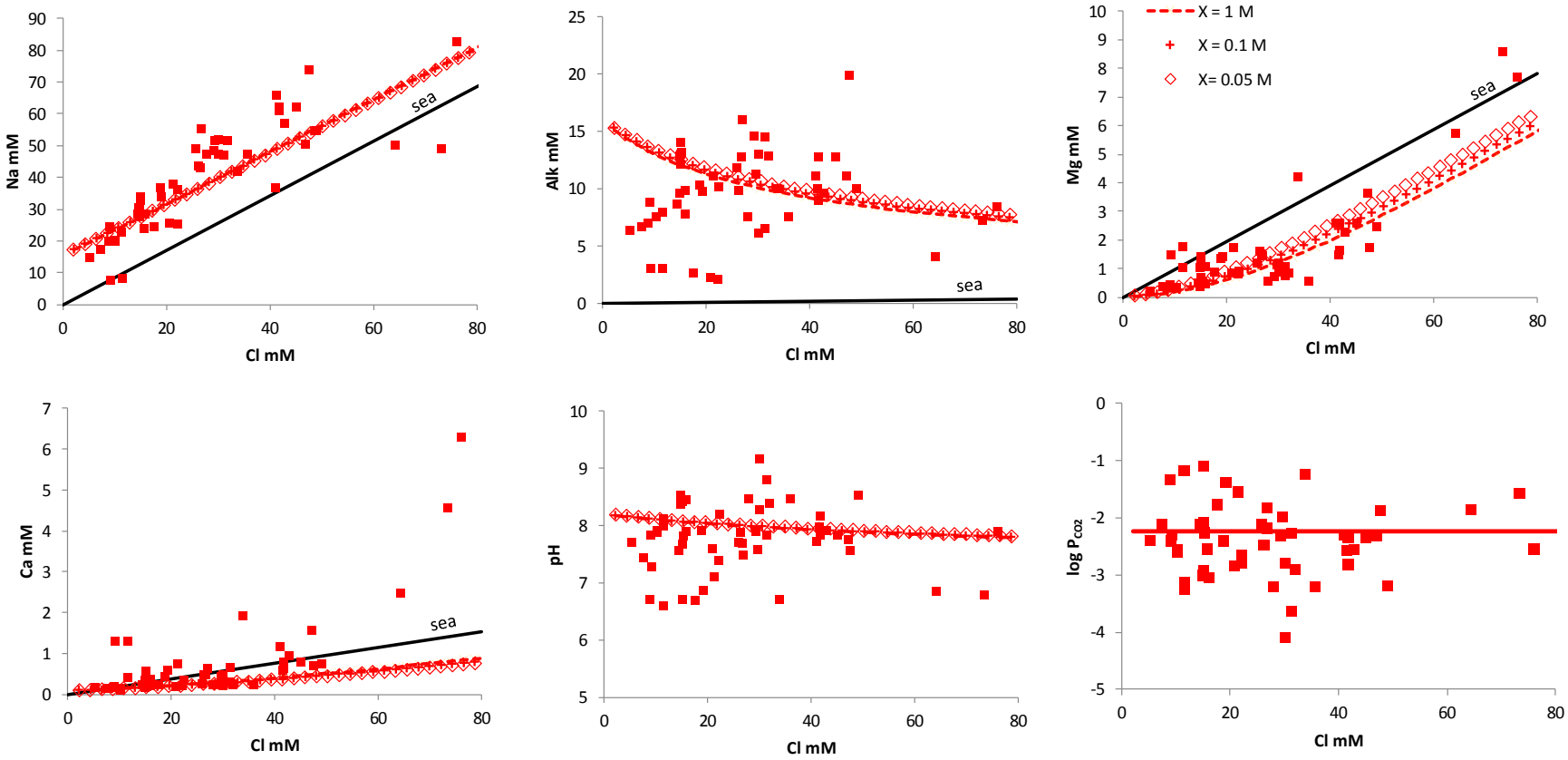

Fig. 8. Groundwater chemistry as compared to the Na/Cl volcanic glass exchange PHREEQC model for three different surface site concentrations with different fitted exchange constants as given in Table 1. Black solid lines indicate the ion/Cl ratio in seawater.

Porto Santo data_dieke_v2_glass.xlsx

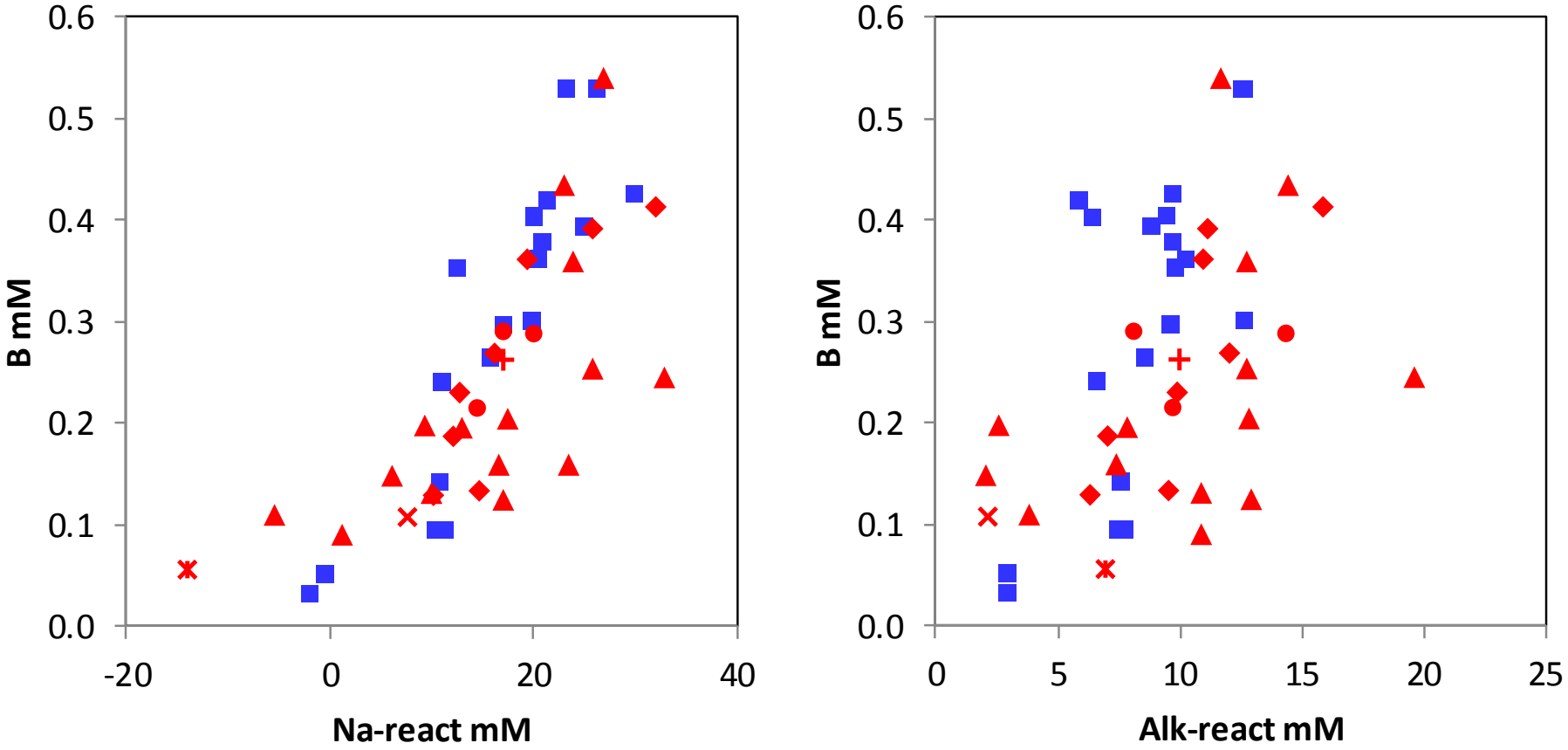

Fig. 9. Boron in groundwater versus the concentrations of Na and alkalinity corrected for their seawater contribution. The seawater contribution is calculated from the ion/Cl ratio in seawater multiplied with the Cl concentration in the groundwater. Blue indicate carbonate aquifer and red volcanic aquifer with a detailed symbol lithology legend presented in Fig. 2c.

Porto Santo data_dieke_v4R.xlsx

- groundwater on volcanic island Porto Santo is high in Na and HCO3 as well as F, B, As and V
- chemistry is controlled by surface leaching of volcanic glass under arid climatic conditions
- geochemical model, based on the surface exchange of Na^+ by H^+ on glass, for the groundwater chemistry

The authors declare no conflicting interests